

# **ELECTROHYDRODYNAMIC PUMPING PRESSURE GENERATION**

A Major Qualifying Project Report:

submitted to the Faculty

of the

WORCESTER POLYTECHNIC INSTITUTE

in partial fulfillment of the requirements for the

Degree of Bachelore of Science

by

*Blair Capriotti*

*Derek Montalvan*

*Michal (Michelle) Talmor*

April 24<sup>th</sup> 2013

Approved:

**Professor Jamal S. Yagoobi, Advisor**

**Professor Eduardo Torres-Jara, Co-Advisor**

## **Abstract**

Electrohydrodynamic (EHD) conduction pumping relies on the interaction between electric fields and dissociated charges in dielectric fluids. EHD pumps are small, have no moving parts and offer superior performance for heat transport. These pumps are therefore able to generate high mass flow rates but high pressure generation is difficult to achieve from these devices. In this Major Qualifying Project, a macro-scale, EHD conduction pump capable of generating up to 400 Pa per section was designed, built and tested. The pump is comprised of pairs of porous, 1.6mm wide high-voltage electrodes with a pore size of 10 $\mu$ m and 3.7mm long flush, ring ground electrodes, spaced 1.6mm apart. The space between pairs is 8mm, with 8 pairs per section. The working fluid is the Novec 7600 engineering fluid.

## **Special Thanks**

We would like to first thank our advisors, Professor Jamal Yagoobi and Professor Eduardo Torres-Jara for providing guidance during the project and for introducing us to the exciting new field of electrohydrodynamics. We would also like to thank Viral Patel and Lei Yang, two of Professor Yagoobi's PhD students, for their immense help with designing, assembling and running the experimental setup described in this report. We would be completely lost without them. We would also like to thank Torbjorn Bergstrom and the rest of the Washborn Shop team for helping us with the manufacturing process for the experimental setup. Lastly, we would like to acknowledge the professional vendors we have had the pleasure to work with: Peterson Steel Inc., Howard Products Sheet Metal, Ultimate Plastics and Mott Corporation.

# Table of Contents

Table of Contents .....	iii
Table of Figures .....	v
Table of Tables .....	vii
Chapter 1: Introduction .....	1
Chapter 2: EHD Pumping Theory.....	2
Overview.....	2
Types of EHD Pumping Mechanisms.....	3
General Pump Design Concepts .....	7
Major Applications of EHD Conduction .....	8
Chapter 3: Autonomous Motion Applications.....	9
Overview.....	9
Microactuators .....	10
Macro-Scale Actuation Devices .....	14
Inspired by Nature.....	15
Locomotion.....	19
Performance & Controllability .....	21
Looking Forward .....	23
Chapter 4: Methodology & Experiment Design .....	24
Overview.....	24
Pressure Estimation Model .....	24
Electrode Selection .....	26
Selection of the Working Fluid.....	27
Design Process .....	30
Final Design .....	33

Experiment Design.....	36
Material Selection .....	37
Manufacturing Process.....	38
Assembly Process .....	42
Final Experimental Setup.....	48
Chapter 5: Results .....	51
Overview.....	51
Pressure Generation .....	51
Power Consumption.....	53
Chapter 6: Discussion .....	54
Overview.....	54
Major Results .....	54
Encountered Issues.....	55
Future Work .....	58
Conclusion .....	59
References.....	60
APPENDIX A: Pump Section Construction Instructions.....	63
APPENDIX B: Final Presentation .....	67

## Table of Figures

Figure 1: Heterocharge Layer Formation .....	5
Figure 2: Conduction Pumping Working Principle .....	6
Figure 3: Generic Pump Design Diagram.....	7
Figure 4: Different Electrode Geometries.....	7
Figure 5: Micromotor Overall Configuration .....	11
Figure 6: Micromotor Rotor Disc Configuration.....	11
Figure 7: Membrane Based EHD Actuator Design .....	12
Figure 8: Heated Fluid Microactuated Membrane.....	13
Figure 9: Micro-Scale Bellows-Based Gripper.....	14
Figure 10: EHD Based Micro-Muscle Expansion .....	16
Figure 11: EHD Micro-Finger Concept of Operation.....	17
Figure 12: Micro-Joint Based on Spider Legs .....	18
Figure 13: EHD Micro-Boat Working Principle .....	19
Figure 14: EHD Propelled, Snail-Like Electroactive Gel.....	20
Figure 15: Electrode and Spacer Design.....	27
Figure 16: Optimistic Pressure Estimations for Different Working Fluids .....	29
Figure 17: Original 12-Electrode Pump Section.....	30
Figure 18: Housing Design Incorporating Endcaps.....	31
Figure 19: Tube Paths between the Nine Pump Sections .....	33
Figure 20: Final Pump Section Design .....	34
Figure 21: Multi Pump Section Housing Cartridge .....	34
Figure 22: Final Pumping Device Design.....	35

Figure 23: LabVIEW Front Panel.....	36
Figure 24: Soft Jaw Clamp .....	39
Figure 25: Example PTFE Endcap Test Piece Manufacturing.....	40
Figure 26: Carving Out & Pre-Tapping the Cartridge .....	41
Figure 27: Drilling Long Holes from Each Side of the Cartridge .....	41
Figure 28: Drilling the Side Holes in the Cartridge.....	41
Figure 29: Pump Section Assembly Using a Cradle.....	43
Figure 30: Weighing Down a Pump Section to Ensure Contact with the Busline .....	44
Figure 31: Assembled Pump Section Inserted into Insulator Housing.....	44
Figure 32: Pass Through Slit for Ground Wire.....	45
Figure 33: Initial Experimental Setup.....	46
Figure 34: Power Supply Wiring.....	48
Figure 35: Experimental Setup Design Diagram .....	49
Figure 36: Final Experimental Setup .....	49
Figure 37: Final Test Results .....	51
Figure 38: Generated Pressure vs. Applied Voltage.....	52
Figure 39: Projected Performance Based on Experimental Data Curve Fit .....	52
Figure 40: Current Usage during Final Test Run.....	53

## **Table of Tables**

Table 1: Microactuator Performance Comparison.....	22
Table 2: Micromotor Performance Comparison.....	22
Table 3: Potential Dielectric Working Fluids .....	28
Table 4: Estimated Pressure Generation from Different Working Fluids .....	28

## Chapter 1: Introduction

Electrohydrodynamics (EHD) is a field of research that studies the interaction between electric fields and fluid flow fields. EHD pumping - the ability to pump specific kinds of fluids via injecting ions into them – has been a known phenomenon for over a century, but rigorous study of it only began in 1959. Over time, different types of EHD pumping have been discovered, with the most recent and most reliable of these being EHD conduction pumping. This type of EHD pumping has thus far been primarily used to enhance the heat transfer capabilities of cooling systems in aerospace applications, relying mainly on the ability of this type of pumping to generate high mass flow rates in coolants with low differential pressures between inlet and outlet. This use of the technology has even matured enough to be approved to be used on the International Space Station starting in 2017. However, EHD conduction pumping has a vast range of potential applications in many other areas of engineering that rely on hydraulic systems as well.

The purpose of this Major Qualifying Project was therefore to investigate the possible use of EHD conduction pumping technology for pressure generation and to realize a proof of concept device that could potentially generate 30 kPa – 50 kPa of differential, static pressure. This utilization of EHD conduction pumping could be used for anything from actuation of robotic devices to flow distribution control in multi-channel systems, or any other applications that require high pressure. This report describes the basic principles of this technology and its uses, as well as the design, fabrication, assembly and testing processes of a proof of concept device capable of pressure generation using EHD conduction pumping.

## Chapter 2: EHD Pumping Theory

### Overview

As mentioned in the introduction, Electrohydrodynamic (EHD) pumping relies on the interaction between electric fields and fluid flow fields. The forces being employed in EHD pumping are the Coulomb force, the dielectrophoretic force, and the electrostriction force. Each of these forces is described by a term in the net body force equation shown below (Melcher, 1981):

$$\vec{F}_e = q\vec{E} - \frac{1}{2}E^2\nabla\epsilon + \nabla\left[\rho\frac{E^2}{2}\left(\frac{\partial\epsilon}{\partial\rho}\right)_T\right]$$

In the above equation,  $F$  is the total body force generated on the working fluid by the application of an electric field.  $q$ ,  $E$  and  $\epsilon$  are the charge density, the electric field strength, and the working fluid permittivity, respectively.  $\rho$  is the mass density and  $\left(\frac{\partial\epsilon}{\partial\rho}\right)_T$  is determined at constant temperature. The first term describes the Coulomb force, the second the dielectrophoretic force and the last term describes the electrostriction term. The latter two require a gradient in permittivity (absent in an isothermal, single phase fluid) and a density changes found in compressible fluids respectively in order to be significantly present.

Electrohydrodynamic pumping is a relatively new field of research. Although initial findings were discovered in the early 19<sup>th</sup> century, it was not until 1959 that experiments were finally conducted to verify the theory. Since then the field has been growing steadily as new applications of the technology are being discovered every day. The following sections describe the three different types of EHD pumping known today, as well as their applications, advantages and disadvantages.

## **Types of EHD Pumping Mechanisms**

There are three different types of EHD pumping: conduction pumping, induction pumping and ion-drag pumping (Seyed-Yagoobi, Electrohydrodynamic Pumping of Dielectric Fluids, 2005). Each of these types generates flow by affecting charges in dielectric fluids by imposing electric fields onto these fluids. Dielectric fluids have very low conductivities (in the range of  $10^{-7} - 10^{-14}$  S/m<sup>2</sup>) and do not have a net charge on their own. Each type introduces charges into the dielectric fluid in a different manner.

Since the only mechanism by which flow is generated in EHD pumping is via the application of an electric field, EHD pumps can operate with no moving parts and their designs can be very simplistic – relying primarily on the geometries of the electrodes used to generate the electric fields. The overall effect is of lightweight, simple mechanisms that require little maintenance and are highly reliable. Since the type of EHD pumping used in this Major Qualifying Project is conduction pumping, this report will describe this type more in depth and only provide a rudimentary description of the other two types.

### **Ion-Drag Pumping**

As its name suggests, this type of pumping requires direct injection of free charges into a dielectric fluid medium. To do so, a sharp corona source, known as an emitter electrode, is used to inject ions and an oppositely charged electrode, known as a collector electrode, attracts them. The flow of ions between the anode and cathode drags the adjacent fluid and causes a net flow to occur. This type of EHD pumping was the first to be investigated by the scientific community and is therefore well documented. However, the biggest downside to this type of pumping is that

it deteriorates and dulls the emitter electrode as more and more of its material is injected into the fluid. In addition, over time the additional charges present in the working fluid damages the unique electrical properties of the dielectric fluid, causing the pumping performance of the to decline and fail. Therefore, although this type of pumping has been studied much more extensively than the other types of EHD pumping and is capable of relatively high pressure generation, its applications have been limited and are undesirable for any device that requires continuous operation (Seyed-Yagoobi, 2005).

### **Induction Pumping**

Induction pumping is a type of EHD pumping that utilizes an electric AC traveling wave in order to attract or repel induced charges in a dielectric fluid medium. As mentioned previously, dielectric fluids do not have a net charge ordinarily, but charges can be induced in them due to a discontinuity of the electric conductivity of the fluid caused by an imposed thermal gradient or change of phase. Therefore, this type of EHD pumping is primarily used in applications where phase changes or significant temperature differences are present. By changing the frequency and voltage of the traveling wave, different flow velocities can be generated in the fluid medium. The concept was initially introduced in the 1990's and has since been investigated further as a way of pumping thin fluid films and combined liquid/vapor phases. However, this type of pumping is unsuitable for isothermal applications (Seyed-Yagoobi, *Electrohydrodynamic Pumping of Dielectric Fluids*, 2005).

## Conduction Pumping

The working principle behind conduction pumping is the interaction between an imposed electric field and dissociated charges within a dielectric fluid. These dissociated charges come from electrolyte impurities already present in the dielectric, which undergo dissociation into ions and recombination back into compounds under an imposed electric field (Seyed-Yagoobi, Electrohydrodynamic Pumping of Dielectric Fluids, 2005).

Under a low strength electric field generated between electrodes submerged in the dielectric, the disassociation and recombination of the dielectric fluid's electrolyte molecules is at equilibrium. However, when the electric field strength is increased past 1-2 kV/cm, the rate of disassociation begins to exceed the rate of recombination and a heterocharge layer comprised of oppositely charged ions forms near each of the electrodes generating the field. The formation of these layers is the mechanism which governs the generated flow. The following image shows the heterocharge layer formation near the surface of submerged electrodes:

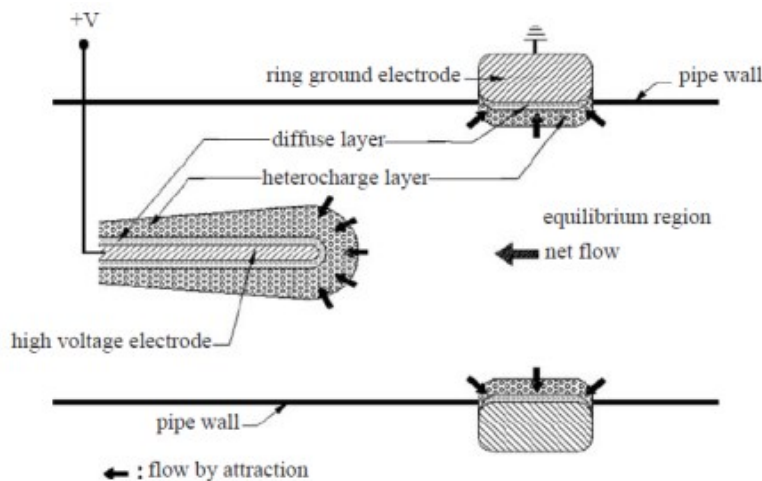


**Figure 1: Heterocharge Layer Formation**  
(Seyed-Yagoobi, Electrohydrodynamic Pumping of Dielectric Fluids, 2005)

In this pumping type, there is no need to generate a discontinuity in the conductivity of the dielectric medium, so the working fluids are regarded as isothermal and incompressible.

Therefore for this type of EHD pumping, the net body force equation reduces to the following:

$$\vec{F}_e = q\vec{E}$$

Note that if the electrodes generating the electric field are symmetric in shape, the negative and positive charge densities cancel out and no net body force is generated, meaning that no flow is generated. Actual pumping flow occurs when the electrodes have a different geometry, which makes for an asymmetrical electric field and a net motion of ions. This principle is illustrated in the image below:

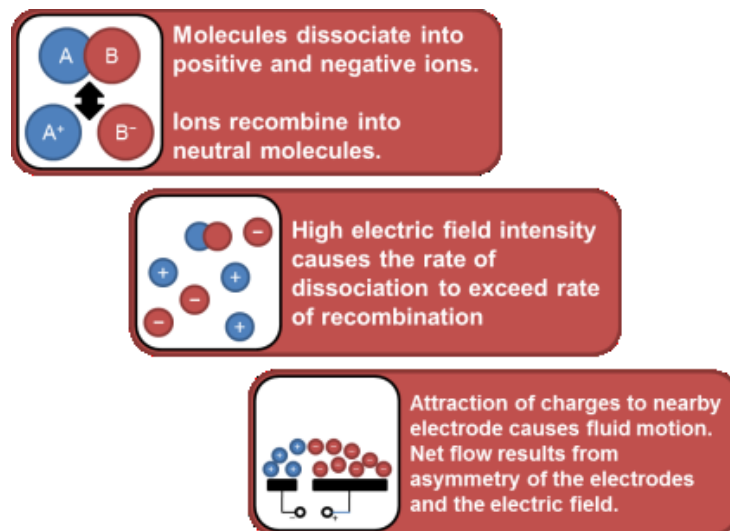


**Figure 2: Conduction Pumping Working Principle**

This type of pumping is the most reliable since no additional heat needs to be applied to the working fluid for the mechanism to work and there is no degradation of the working fluid due to additional ions being injected into it. In addition, although this type of pumping requires relatively high input voltages, the current consumption of EHD conduction based devices is very low, in the sub-ohmic regime (Seyed-Yagoobi, 2005).

## General Pump Design Concepts

The image below illustrates a generic pump design for EHD conduction pumps:

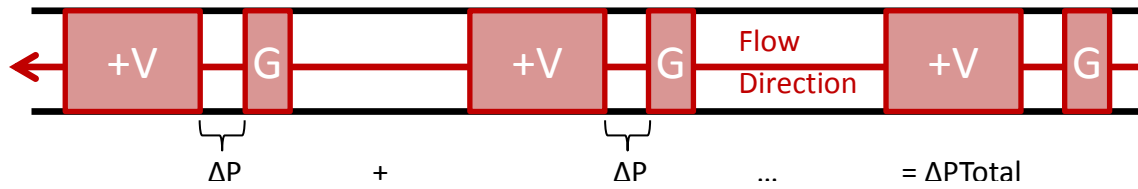


**Figure 3: Generic Pump Design Diagram**

In the above image, several electrode pairs are placed within a flow channel. The spacing between the high voltage (+V) electrodes and the ground electrodes (G) is carefully specified based on the electrode dimensions in order to achieve the most performance out of the imposed electric field. In many EHD applications, the width of this space is the same as the width of the thin ground electrode, with the high-voltage electrode being three times as wide - (Pearson & Seyed-Yagoobi, 2011) for instance. The space between the electrode pairs is usually the minimum space required for their generated electric fields not to interfere with each other. Usually, this width is five times the width of the thin ground electrode. The electrodes themselves can have many shapes, as illustrated below:

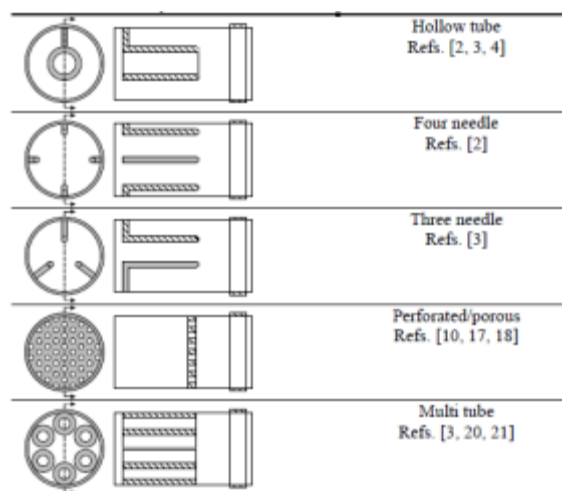


**Figure 4: Different Electrode Geometries (Pearson & Seyed-Yagoobi, 2008)**

Different electrode designs can be used for different applications, depending on which characteristics of the flow are of interest (pressure, mass flow rate, etc). Higher pressures can be generated via adding electrodes or pump sections in series, as the above image illustrated, since the effects of the net body force generated between each electrode pair add together nearly linearly for electrodes in series (Jeong & Seyed-Yagoobi, 2002).

## **Major Applications of EHD Conduction**

EHD conduction technology has been very successful thus far in improving the heat transport properties of cooling systems that use refrigerants (Seyed-Yagoobi, *Augmentation of Two-Phase and Single-Phase Heat Transfer and Mass Transport with Electrohydrodynamics in Thermal Equipment*, 1999). For instance, it has been shown that EHD is able to continue to wet the evaporator interface with coolant past when it would otherwise dry out and thereby increase the heat transfer capability of the evaporator (Pearson & Seyed-Yagoobi, 2011).

EHD conduction pumping has also been successful at pumping thin fluid films, which can be used to pump vapor phases that can be carried by an EHD driven liquid phase (Pearson & Seyed-Yagoobi, *Advances in Electrohydrodynamic Conduction Pumping*, 2008). EHD has also shown to work well in micro-gravity (Robinson, Patel, Seyed-Yagoobi, & Didion, 2012), making it a very attractive technology for use in space.

However, not much research has been performed regarding other applications of EHD technology in general, and conduction pumping in particular, as it is a relatively new field. The next section will offer a review of one area of research which shows great promise for the technology – autonomous actuation.

## Chapter 3: Autonomous Motion Applications

### Overview

EHD conduction pumping appears at first glance to be a relatively simplistic technology with limited success beyond the field of heat transfer. However, since the core principal of the technology is the interaction between electrical fields and fluid flow fields, the actual range of possible applications for this technology includes within it all uses that normally fall under the field of hydraulics. Therefore, many common applications that rely on the control of fluid pressure and mass flow rate can stand to benefit from EHD technology.

It is therefore not surprising to find that the scientific community has already made efforts to eke out further uses for this technology, especially as it pertains to autonomous actuation. Since EHD performance only increases as the scale of it is reduced, much of the focus of the aforementioned research has been in the field of microactuation for micro-scale robotics or medical applications. In addition, since EHD output is directly related to the strength of the applied electric fields, with extremely fast response rates – on the order of milliseconds (Feng & Seyed-Yagoobi, Control of Liquid Flow Distribution Utilizing EHD Conduction Pumping Mechanism, 2004), EHD conduction pumping can be reliably used in applications that require exact control.

This section offers a review of the major different applications currently being researched for EHD conduction pumping that involve actuation for autonomous devices. A review of the performance of these devices and how they compare to similar, mundane hydraulic devices is also presented here, as well as a projected estimate for the next steps of development for this type of application of EHD conduction pumping technology.

## **Microactuators**

Since EHD devices perform better when down-scaled, the majority of development of EHD devices for the purpose of autonomous actuation has been in the micro scale. With no moving parts and simple designs that can be easily manufactured, even as simple electric circuits on both solid surfaces and flexible materials (Chen, Selvarasah, Chao, Khanicheh, Mvroidis, & Dokmeci, 2007), microactuation seems like a perfect application for this technology. In addition, micro-scale EHD devices require much lower applied voltages, making them far more attractive power-wise than their larger equivalences. Some EHD-based microactuators that have been researched thus far include micromotors and elastic membrane actuators (De Volder & Reynaerts, 2010). However, many other types of hydraulic microactuation could be converted to using dielectric fluids and therefore benefit from EHD conduction as well. The following subsections describe the major existing developments in EHD microactuation as well as other hydraulic microactuation applications that could benefit from EHD technology.

### **Micromotors**

An example micromotor was proposed and tested by Yokota et al in 2005. This motor was comprised of a thin shaft that was inserted into a rotor made of several discs. The rotor was placed in a sealed container filled with dielectric fluid with a bearing that allowed the shaft to rotate. Each disc was made of four layered sub-discs. The outer two contained the actual electrodes that would interact with the fluid and the two internal ones formed the busline connections to the electrodes. The electrodes were arrayed in a 2D windmill-like configuration, as can be seen on the next page.

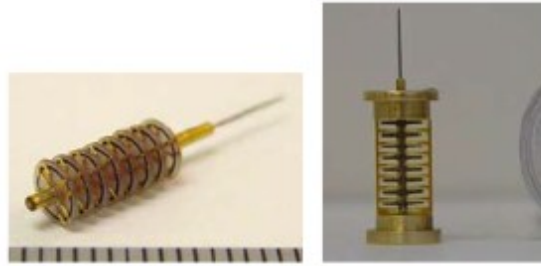


**Figure 5: Micromotor Overall Configuration (Yokota, Kawamura, Takemura, & Edamura, 2005)**

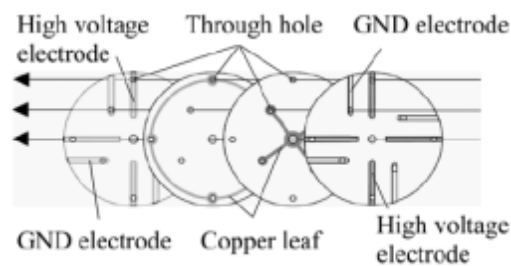


**Figure 6: Micromotor Rotor Disc Configuration (Yokota, Kawamura, Takemura, & Edamura, 2005)**

As can be seen in the image above, the windmill configuration of the electrodes was very simple, with straight asymmetrical electrodes. A force perpendicular to the orientation of each electrode pair propels the disc to rotate. Since the effects of EHD conduction are additive, adding several such discs to the shaft that can rotate together increased the output torque of the device significantly. Miniaturization this device had interesting results as well, since although the forces generated by the EHD conduction phenomenon were stronger, the overall moment arm about the shaft was shortened. This resulted in an overall reduction of output torque, but still a significant increase in output torque and output torque densities (to a range of 78-85 Nm/m<sup>3</sup>) and output power densities, implying that for the space saved with miniaturization multiple such devices could be added together for an overall torque increase (Yokota, Kawamura, Takemura, & Edamura, 2005).

## Membrane Microactuators

Kashani et al proposed a new microactuator design that was based on the displacement of a thin membrane separating between two fluid chambers filled with in a dielectric fluid. Fluid would be pumped from one chamber to the other via an adjoined EHD pump section and would cause the membrane to displace. The stroke length of the membrane would be controlled by the applied voltage on the pump, as illustrated below:

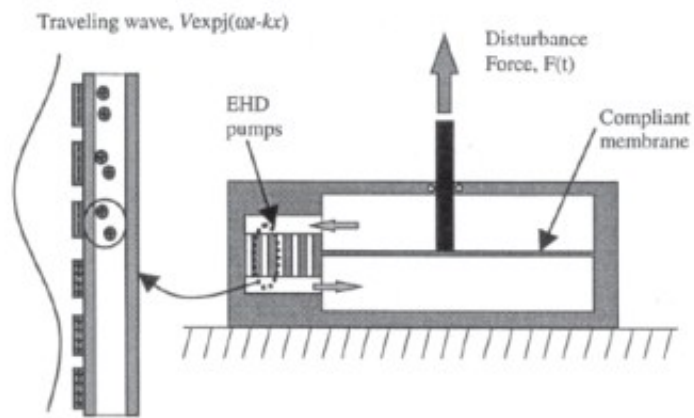


**Figure 7: Membrane Based EHD Actuator Design  
(Kashani, Kang, & Hallinan, 2000)**

The actuator could be made to oscillate continuously as well, via simple continuous variations of the input voltage.

However, there is much hidden potential in the field of membrane-based actuators for EHD to fulfill. Currently many membrane-based micro-valve systems operate on a thermal expansion principle, in which a heater causes a fluid medium to expand or contract within an enclosing membrane (De Volder & Reynaerts, 2010). An example of such a mechanism can be seen on the following page.

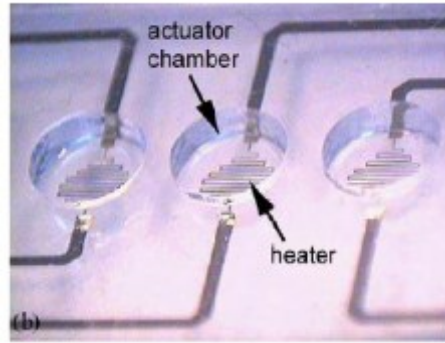


**Figure 8: Heated Fluid Microactuated Membrane  
(Jeong, Park, Yang, & Pak, 2005)**

Yet in situations where heat must be carefully controlled, EHD technology with its low levels of Joule heating and ability to generate pressure without the application of heat may be more beneficial.

### **Other Potential Microactuation Devices**

There are many other types of hydraulic micro-actuators that could stand to benefit from EHD technology. These are generally divided into elastic micro-actuators and micro-mechanical actuators. Elastic microactuators involve an elastic container, such as a membrane or a balloon that can be made to grow, shrink or move by manipulating the fluid within the container. Micro-mechanical devices, in contrast, are simply miniaturized versions of macro-scale mechanical devices, such as piston-based actuators (De Volder & Reynaerts, 2010).

Thus far, EHD conduction technology has only been applied to a limited number of elastic and micro-mechanical hydraulic actuators, but the basic principles of the technology could be applied to essentially all such types of microactuators. For instance, as in the case of the membrane micro-valves described above, creating valves or joints based on the expansion and contraction of an elastic balloon micro-actuator that does not use heat as the main source for the

actuation could be beneficial. Similarly, miniaturized elastic bellows-type devices, such as the three-bellows micro-gripper suggested by Kang et al in 2006, which can be seen below, could be developed and enhanced with EHD conduction technology as well, allowing for controllable, autonomous linear motions in the micro-scale that could be used for accurate grippers, slider mechanisms and more.

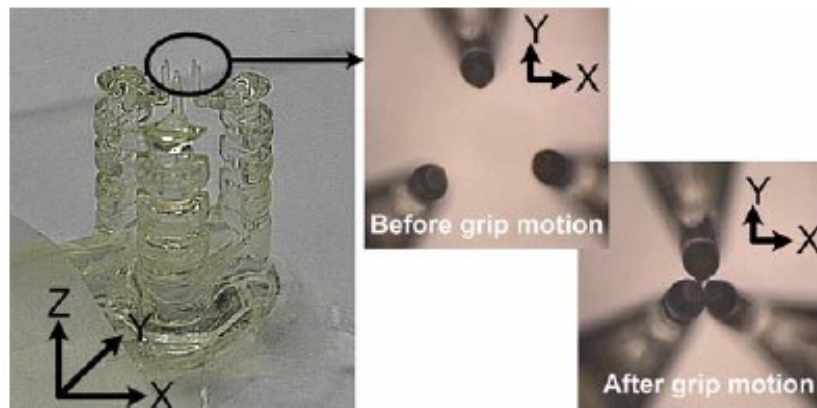


**Figure 9: Micro-Scale Bellows-Based Gripper  
(Kang, Lee, & Cho, 2006)**

For micro-mechanical devices, which are primarily based on increasing and reducing pressure in order to actuate a mechanical mechanism, EHD pressure generators such as the one described in this report could be used, if miniaturized. Thus far, however, no work seems to have been done to investigate such potential devices.

## **Macro-Scale Actuation Devices**

In the case of electrohydrodynamic conduction, macro-scale actuation does not imply macro-scale pumping devices. Indeed, whereas macro-scale and meso-scale devices are only able to achieve pressures in the region of 125 Pa (Pearson & Seyed-Yagoobi, Experimental Study of EHD Conduction Pumping at the Meso- and Micro-Scale, 2011), micro-scale devices

are able to achieve as much as 1.37 kPa of pressure between a single pair of electrodes (Jeong & Seyed-Yagoobi, 2004).

That said, since pressure generation and mass flow rate grow approximately linearly (Jeong & Seyed-Yagoobi, 2002) when EHD pumps are connected together in series, it is possible to add several small micro-scale devices together to achieve a power output that is equivalent to other types of commercially available devices, such as piezoelectric and magnetostrictive actuators (Kashani, Kang, & Hallinan, 2000). Overall, since the individual EHD actuator sizes would be so small, it would result in a composite device no larger than commercial macro-scale pumps, but with all the advantages of miniaturized EHD technology (no moving parts, simple operation, increased power density etc.).

However, even though each miniaturized EHD device would not need much input voltage and would use very little current, several such devices added together could become costly, power-wise. Unfortunately, not much research has focused on optimizing the power consumption of composite, macro-scale EHD devices. Therefore, they still remain a theoretical concept that might be usable after further research.

## **Inspired by Nature**

Thus far this section has focused primarily on actuators based on purely mechanical devices – pumps, valves, motors and linear actuators. However, science and engineering have always taken great inspiration from the more dynamic motions found in nature – from Leonardo Da-Vinci’s fascination with flight and the study of bird wings all the way to modern, insect-like multi-legged robotics. Therefore, the ability to manufacture micro-scale or even nano-scale

hydraulic devices that can actuate using natural motion can be very beneficial to a wide range of technologies in development, especially for robotic and medical applications. For instance, hydraulic micro-muscles can be used to make strikingly life-like robots for human-machine interaction or robotic prosthetics that move and feel like their organic equivalent. Advancement in this field have mostly been made using McKibben actuators (De Volder & Reynaerts, 2010), which require an external pump to operate, but which have a very attractive force outputs. The advantage of EHD devices over these, however, is in that EHD devices do not require any external pumping device to work.

A design for such an EHD conduction based micro-muscle has already been proposed by Takemura et al in 2005. This micro-muscle is constructed of a flexible cylindrical container with a structure that forces it to contract in the axial direction and expand radially when the pressure of the fluid contained within it rises. The following image shows the expansion of such a micro-muscle with twelve aramid fiber “ribs” that divide its expansion to twelve different sections arrayed in a close-knit circle:

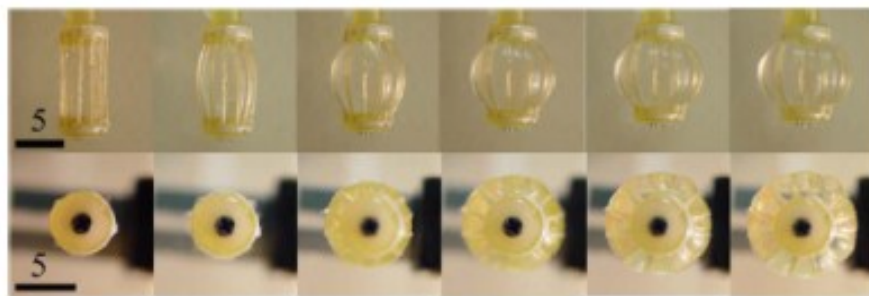


**Figure 10: EHD Based Micro-Muscle Expansion  
(Takemura, Yokota, & Edamura, A Micro Artificial Muscle Actuator Using Electro-Conjugate Fluid, 2005)**

A big advantage of this micro-muscle design is that it was very easily manufactured out of silicone rubber and does not leak even when a relatively high pressure is applied to its walls

by the dielectric fluid within it. As the image shows, the expansion of this micro-muscle was actually relatively large for its size and the force it could apply to an object was 0.18 N at 6kV of applied voltage on a single pair of electrodes (Takemura, Yokota, & Edamura, A Micro Artificial Muscle Actuator Using Electro-Conjugate Fluid, 2005), which is relatively high for a device only 5 mm in diameter and 35 microns thick. Improvements to this device could be made by adding more electrodes and adding several such devices together to make a composite muscle, as was shown by the same group three years later (Takemura, Yajima, Yokota, & Edamura, 2008).

Another example of a very simple composite muscle is the micro-scale finger that was proposed and tested by Abe et al in 2006. The finger is comprised of three chambers similar to the micro-muscle tube shown above, but without the fiber ribs. Each chamber is filled with the dielectric medium fluid and is controlled by a single electrode pair. The finger can then bend in different directions based on which electrodes are active at any given point in time. The image below shows the basic concept of operation for this micro-finger:

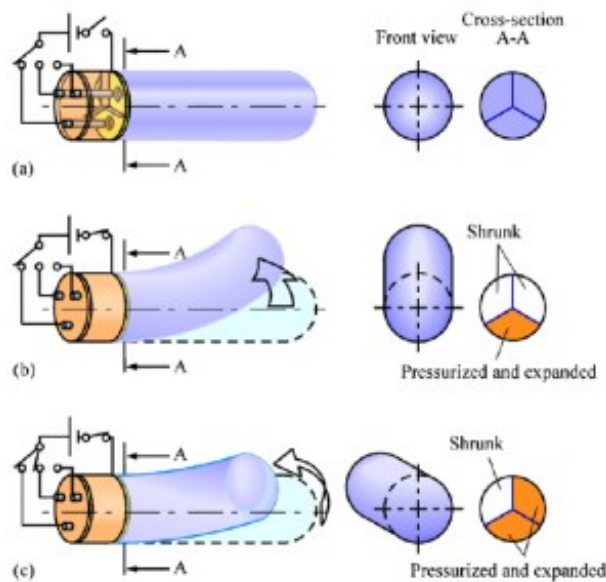


**Figure 11: EHD Micro-Finger Concept of Operation (Abe, Takemura, Edamura, & Yokota, 2006)**

This finger did not prove to be as flexible as was hoped since fluid could not be transferred out of chambers that were not actuated, but with a simple mechanism of flow distribution control it could easily be modified to evacuate fluid out of the unused chambers and move it to the activated ones (Feng & Seyed-Yagoobi, Control of Liquid Flow Distribution Utilizing EHD Conduction Pumping Mechanism, 2004). Such a micro-scale finger has great potential to be used as an intuitive, remotely controlled gripper that moves as human fingers do but can manipulate small objects in hard-to-reach locations.

Both of the above examples show promise for the replication of general muscle-like and appendage-like motion. However, EHD conduction technology can also aid in simple micro-joint applications that simulate other life-like motions. The prime example for this is pneumatic joints capable of replicating the joints in a spider's legs. Spider legs are actuated entirely by pressurizing a special membrane found at their joints using their blood as the working fluid. When this membrane is pressurized, the leg bends and when it is de-pressurized, the leg straightens again (De Volder & Reynaerts, 2010). Menon and Lira proposed and tested a hydraulic microactuator capable of replicating this motion, which can be seen below:

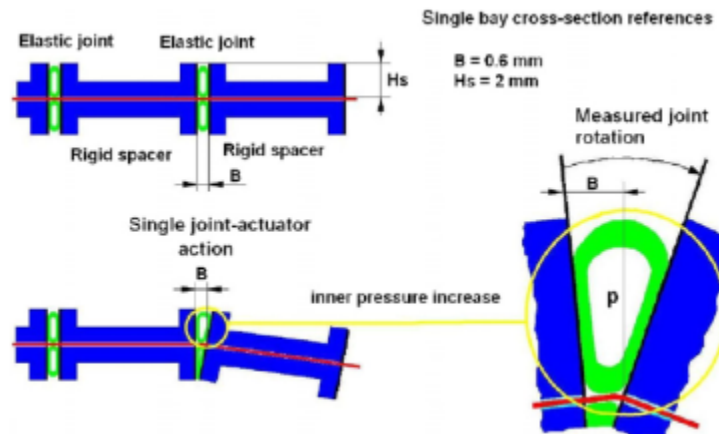


**Figure 12: Micro-Joint Based on Spider Legs (Menon & Lira, 2006)**

Although this microactuator was not originally designed to use the EHD conduction phenomenon, adapting it to use it would be relatively easy. In addition, this microactuator was designed specifically for space applications, so the space-worthy technology of EHD conduction pumping would be compatible with its planned use.

## Locomotion

Another interesting new field of research on EHD conduction phenomenon focuses on creating autonomous devices capable of locomotion using only an applied electric field on a dielectric medium as their means of propulsion.

Wang et al proposed and tested a micro-scale boat comprised of an EHD pump circuit printed on the bottom of a thin parylene sheet 1cm x 1.5cm in size. With the electrodes facing down, the boat could theoretically propel itself forward due to the net body force that would be generated between each electrode pair. The working principle of this device is shown below:

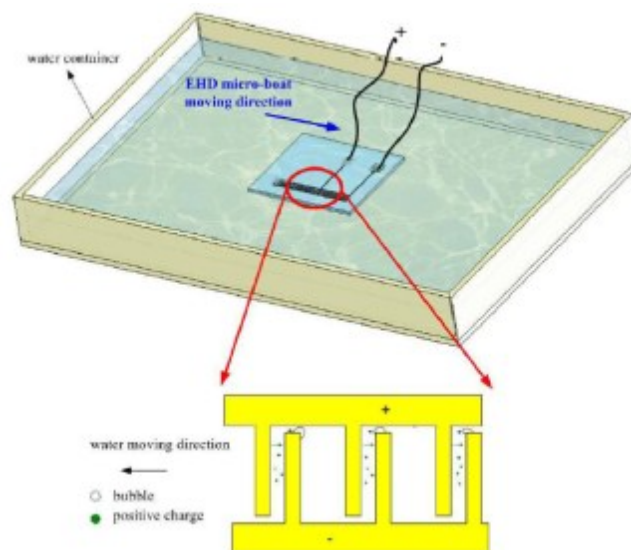


**Figure 13: EHD Micro-Boat Working Principle (Wang, Lin, & Yang, 2007)**

However, in this particular case the fluid chosen for the boat to ride upon was water, despite it having too high a conductivity for the EHD conduction phenomenon to work properly. The concept behind this choice was to use the bubbles created during the electrolysis of the water beneath the boat to propel the boat. However, the results were a very slow movement rate across the water - 6.5mm per minute (Wang, Lin, & Yang, 2007). Had the boat been tested over a dielectric fluid, its performance would have likely been much better.

A more successful example of another locomotive application that did opt to use a dielectric fluid is the autonomous snail-like device proposed by Liang et al in 2007. For this application an electroactive polymer (EAP), which changes its shape when an electric field is applied to it, was created from PVA gel swollen with a dielectric working fluid and shaped into a thin snail-like strip. The work plane for this device is a glass surface with two electrodes at either end (anode and cathode). A path is cast onto the workplace by applying a bit of the dielectric working fluid onto it in the desired path shape. Setting the gel snail down near the anode at the beginning of the path and activating the electrodes causes the snail to quickly crawl along the path to the cathode. At 6 kV the snail achieved a rather speedy velocity of 4.8 mm/s (Linag, Xu, Weng, Zhang, Guo, & Zhang, 2007). The working principle of this device can be seen below:

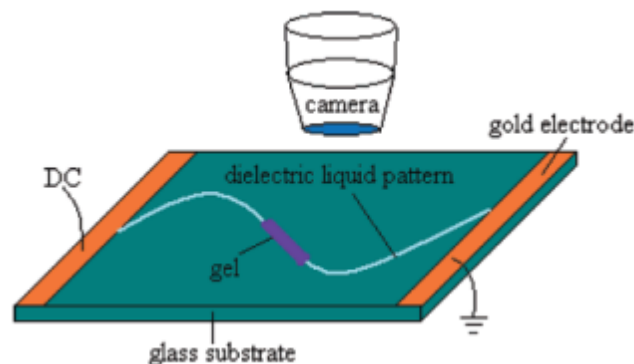


**Figure 14: EHD Propelled, Snail-Like Electroactive Gel (Linag, Xu, Weng, Zhang, Guo, & Zhang, 2007)**

The main issue with this application is that the snail loses some of its mass as the dielectric fluids it is swelled with flows out during its motion, thereby slowly rendering it incapable of continuous motion. However, since the main mechanism of this locomotion is just the motion of charges from one electrode to the other, without a need for a net flow of the fluid, this application can use symmetric electrodes whose charge can be reversed in order to “back-drive” the snail back to its start position along the same path.

## **Performance & Controllability**

As was mentioned previously, the response time of EHD conduction based devices is very fast and, since there is no degradation of the electrodes or the working fluid, such devices are very reliable in continuous operation and their behavior is highly predictable and repeatable (ref?). Because of this, EHD conduction based hydraulics is especially attractive for high-precision applications.

However, the application of this technology to actuation and motion control is still very much in its infancy. In order to understand where the applicability of autonomous actuation using EHD conduction stands, its overall performance must be evaluated and compared to other existing solutions. The tables on the following page therefore compare first between general microactuators (De Volder & Reynaerts, 2010) and some of the EHD-based microactuators described previously, and second between the micromotor described previously and a commercial piezoelectric micromotor (PiezoMotor).

<b>Actuator Type</b>	<b>Operating Pressure</b>	<b>Output Force</b>	<b>Stroke Length</b>	<b>Cross-Section Size</b>
<i>Micro-Piston</i>	1.5 MPa	1 N	10 mm	1.3 x 13 mm
<i>McKibbean</i>	1 MPa	6 N	8 mm	1.5 x 62 mm
<i>EHD Artificial Muscle</i>	10 kPa	0.2 N	1.6 mm	5 x 10 mm
<i>EHD Micro-Finger</i>	8 kPa	0.9 mN	7.2 mm	4.5 x 30 mm

**Table 1: Microactuator Performance Comparison**

<b>Motor Type</b>	<b>Rotational Velocity</b>	<b>Output Torque</b>	<b>Power Consumption</b>	<b>Size</b>	<b>Operating Voltage</b>
<i>9mm ID EHD Micromotor</i>	46.5 rad/s	50.8 $\mu$ Nm	0.6 mW	11 x 14 mm	6 kV
<i>5mm ID EHD Micromotor</i>	93.4 rad/s	16.3 $\mu$ Nm	0.4 mW	7 x 14 mm	6 kV
<i>Piezoelectric Micromotor</i>	0.33 rad/s	90 mNm	7.5 mW	23 x 34 mm	48 V

**Table 2: Micromotor Performance Comparison**

As can be seen in the first table, although the EHD artificial micro-muscle and micro-finger both operate under much lower pressures, their output force leaves much to be desired. In the case of the micro-finger, the stroke length was comparable to that of the more conventional microactuators. However, considering the specific principle of operation of the artificial micro-muscle, its relatively short stroke is not surprising. As a trade-off, it is clear that the micro-muscle is able to output a much higher force than the micro-finger, especially considering its significantly smaller size. Neither, however, is likely sufficiently mature to replace the other actuators in the next few years.

From the second table, it is clear to see that although the EHD-based motors require a much higher operating voltage and produce significantly less output torque, they are capable of achieving greater rotational velocities, consume much less power and are significantly smaller

than standard piezoelectric motors. In addition, Takemura et al have estimated that if the micromotor they proposed can be reduced further in size such that the applied electric field can be up to ten times greater than what they had observed, the output torque density of this smaller micrometer would be enough for it to not only meet the power density of existing piezoelectric and magnetostrictive actuators, but even exceed it (Takemura, Kozuki, Edamura, & Yokota, 2007). Therefore, for the second table at least we may see great improvement in the near future.

## **Looking Forward**

Based on the performance estimates shown in the previous sub-section, it can be seen that using EHD conduction pumping for the purpose of autonomous motion control shows great promise, but is not sufficiently mature at present. Further optimization, especially in the areas of the required voltage supplies and the expected output forces, is necessary before these types of devices can be commercially produced.

However, as each of the previous sub-sections have shown, there is still a lot of room for EHD conduction technology to expand to, especially in the area of nature-inspired, flexible hydraulics. It is therefore possible that in the future we may be able to fully utilize this technology in robotic micro-joints in life-like appendages or muscle structures. On the rigid actuation side, simple pressure generating devices like the one proposed in this report could be used to actuate mechanical parts of larger devices, especially for space applications since the technology has already been proven to work in such an environment.

## **Chapter 4: Methodology & Experiment Design**

### **Overview**

As stated in the introduction to this report, the main challenge of this Major Qualifying Project was to fabricate an EHD conduction pump capable of generating 0.3-0.5 atmospheres of differential pressure using a dielectric working fluid. However, there were additional requirements from this device:

- The pump device must be as small and lightweight as possible
- The pump device must be safe to operate with a chosen working fluid
- The overall assembly must be able to withstand high operation pressures
- The design must be simple to manufacture and assemble
- The device must be able to be taken completely apart and put back together repeatedly
- Manufacturing of this design must use as little outside resources as possible
- The pump device should have the option to switch between static pressure generation and pressure generation with a significant mass flow rate
- The pump device should be modular, allowing for future additions to the design

These requirements were met over the course of an iterative design process that yielded the final EHD conduction pumping device described in the following sub-sections.

### **Pressure Estimation Model**

In order to come up with a consistent, working design for a pumping device based on EHD conduction, it was beneficial to research previous EHD pumps that were able to generate

pressure. The most prominent published work in the area of pressure generation using the EHD conduction phenomenon is the work of Jeong et al, who initially discovered that high voltage electrodes comprised of multiple tubes were better able to generate pressure than other geometries (Jeong & Seyed-Yagoobi, 2002). Continuing to experiment with other electrode geometries, Jeong et al discovered that perforated and permeable porous high voltage electrodes offered even better pressure generation performance, depending on their hole or pore size (Jeong & Seyed-Yagoobi, 2004).

Feng et al did a full numerical analysis on pressure generation using the EHD conduction phenomenon and then compared it with tests done on perforated electrodes using R-123 as the working fluid (Feng & Seyed-Yagoobi, Understanding of Electrohydrodynamic Conduction Pumping Phenomenon, 2004). The results of the numerical pressure generations are:

$$\Delta P = 0.85m\epsilon \frac{V^2}{d^2} \quad \textit{upper bound}$$

$$\Delta P = 0.5m\epsilon \frac{V^2}{d^2} \quad \textit{lower bound}$$

Where  $m$  is the number of electrode pairs,  $\epsilon$  is the fluid permittivity,  $V$  is the applied voltage, and  $d$  is the spacing between the high-voltage and ground electrodes. The upper bound equation is for a generic, flush high-voltage electrode, whereas the lower bound equation takes the degree of “openness” of a perforated or permeable electrode into account – the space taken up by the holes or pores. The experimental data gathered by Feng et al was between the above two estimates, but lay closer to the lower bound one. These formulas were used in conjunction with the working fluid parameters in order to estimate the desired number of electrode pairs for this project.

## Electrode Selection

At this point in the project, it was established that the best electrode configuration for high pressure generation was a combination of a permeable porous high voltage electrode to generate the high pressure and a flush ring ground electrode to allow the high voltage to control the pressure generation without interference (Jeong & Seyed-Yagoobi, 2004). For the pore size, a size of 10  $\mu\text{m}$  was selected. In the work by Jeong et al both 40  $\mu\text{m}$  and 0.2  $\mu\text{m}$  permeable porous electrodes were studied. Since we wanted to improve upon the performance of the 40  $\mu\text{m}$  electrodes, we needed a smaller pore size. However, at a pore size of 0.2  $\mu\text{m}$ , very little flow rate is generated. In the event that future study of the mass flow rate and other flow properties of the pumping device proposed in this report would be desired, a pore size that would be large enough to allow for some flow would be required. Lastly, the vendor for the electrodes, Mott Corporation, only had 5  $\mu\text{m}$  and 10  $\mu\text{m}$  permeable stainless steel discs in stock.

The spacing between the electrodes was also governed by the size of the high voltage electrodes that were commercially available. Originally, the width of the high-voltage electrode was designed as 1mm. However, only 1.56mm wide electrodes were available for sale. Therefore, the ground electrodes and inter-electrode spaces had to be adjusted as well. Based on the aforementioned work by Jeong et al, the ratio of widths between the high-voltage electrodes and the ground electrodes was set at 1:2.3, with the space between the high-voltage and the ground electrodes set to the width of the high voltage electrode. Note here that every part of either electrode had to be at least 1.56mm from the other electrode, which is why the electrodes have a large gap on one side of them – to allow for the other electrode's busline to be placed without being too close to the oppositely charged electrodes. The space between electrode pairs

was had at a ratio of 1:5 to the width of the high-voltage electrode. The final electrode designs, as well as the designs for the insulating spacers between them, can be seen below:

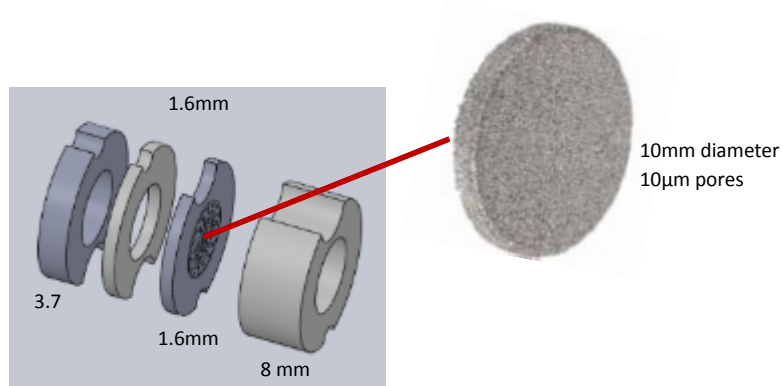


**Figure 15: Electrode and Spacer Design**

As the image above shows, the permeable porous electrodes are simple discs 10mm in diameter. In order to avoid damaging these electrodes when trying to connect them to the high-voltage buslines and in order to utilize as much as their surface area for active pumping as possible, a stainless steel housing was designed for them. The electrodes themselves are embedded in this housing and maintain a good electrical contact with it. Any busline connections can therefore be made to the housing, rather than the sensitive electrodes.

## **Selection of the Working Fluid**

With the electrode designs finalized and knowing that a pressure estimation model based on Feng et al's predictions of generated pressure, a trade study between several different potential working fluids could be conducted. The table on the following page shows a comparison between the dielectric fluids that were considered as potential working fluids (American Society of Heating, 2005). The main parameters of importance are the dielectric constant which governs the fluid permittivity used in the pressure estimation, the boiling point

which controls how safe it is to work with the fluid and the dielectric strength which governs how much voltage can be applied onto the electrodes in the pumping device.

<b>Fluid Name</b>	<b>Dielectric Constant</b>	<b>Conductivity [S/m]</b>	<b>Density [kg/m<sup>3</sup>]</b>	<b>Boiling Point [C°]</b>	<b>Dielectric Strength [kV/mm]</b>
<i>HFE- 7600</i>	6.4	3.33E-08	1540	98	31
<i>HFE-7100</i>	7.4	7.0E-10	1520	61	11
<i>R-123</i>	4.8	2.7E-8	1464	27	25
<i>R-134a</i>	9.51	5.65E-11	1233	-26	18

**Table 3: Potential Dielectric Working Fluids**

To properly compare between these fluids, the aforementioned estimation model for pressure generation was used to generate the table below. In order to make a realistic estimation of the pressure that could be generated from each of the above fluids, the percent porosity of the high voltage electrodes that were selected had to be estimated as well. Since the chosen electrodes were highly porous, a porosity percent range of 82% to %87 was assumed, giving an upper and lower bound for the generated pressure estimates shown below.

<b>No. of Electrodes</b>	<b>R-134a Pressure [Pa]</b>		<b>R-123 Pressure [Pa]</b>		<b>HFE-7100 Pressure [Pa]</b>		<b>HFE-7600 Pressure [Pa]</b>	
	<i>Upper</i>	<i>Lower</i>	<i>Upper</i>	<i>Lower</i>	<i>Upper</i>	<i>Lower</i>	<i>Upper</i>	<i>Lower</i>
20	26469	20241	11866	10284	9773	8470	15717	13622
30	39704	30362	17799	15425	14660	12705	23576	20433
40	52938	40482	23731	20567	19546	16940	31435	27244
50	66173	50603	29664	25709	24433	21175	39294	34055
60	79408	60724	35597	30851	29320	25410	47152	40865
70	92642	70844	41530	35993	34206	29645	55011	47676
80	105877	80965	47463	41135	39093	33881	62870	54487

**Table 4: Estimated Pressure Generation from Different Working Fluids**

The data in Table 4 was calculated based on an applied voltage of 15 kV for all fluids since that is a very standard voltage limit for EHD-based experiments, except for HFE-7100 for which 11 kV was used since that is its breakdown voltage. The highlighted regions denote the entries that fall within the desired pressure generation range for this Major Qualifying Project. Although generating even more pressure would be beneficial, it was considered outside of the scope of this project. This information is also summarized in the following graph, for the upper bound (optimistic estimate):

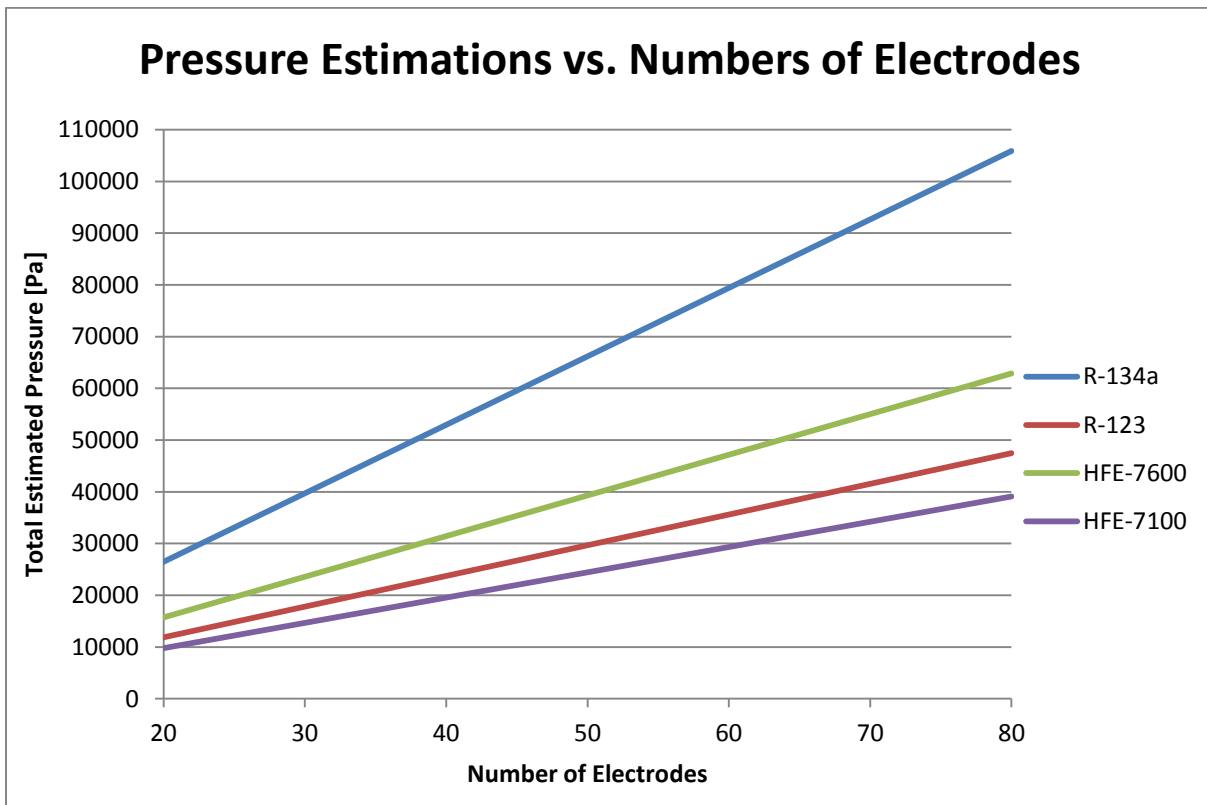


**Figure 16: Optimistic Pressure Estimations for Different Working Fluids**

From the two tables on the previous page, it can be seen that although R-134a has the largest dielectric constant and therefore the highest estimated generated pressures, as well as a decent dielectric strength, its low boiling point means it needs to be highly pressurized in order to remain in a liquid state. It is also considered a very hazardous material and is therefore not a

safe option. HFE-7100 has a high dielectric constant as well, but its low dielectric strength means it has the lowest overall potential for pressure generation. A good mid-ground between the two is HFE-7600, also known as Novec Engineering Fluid 7600, with its decent dielectric constant and very high dielectric strength. This fluid was therefore chosen as the working fluid for the pump design described in this report.

From the graph, it can be seen that a minimum of about 40 electrodes or so would be needed to generate 0.3 atmospheres and about 60 to generate 0.5 atmospheres of differential pressure. The final number of electrodes chosen was 72, constituting a safety factor of 1.2.

## Design Process

After the electrode configuration was determined with the proper spacing and the number of electrodes was finalized, the configuration of the pumping device had to be designed as well.

Since arraying 72 electrodes and their spacers in one long pump would create a very long device (~1m in length) that had no modularity and would be difficult to handle and store, it was decided to divide the electrodes into separate pump sections that would be connected in series via tubes. Originally, each pump section was designed to have twelve electrode pair in sequence. An image of this original design can be seen below:

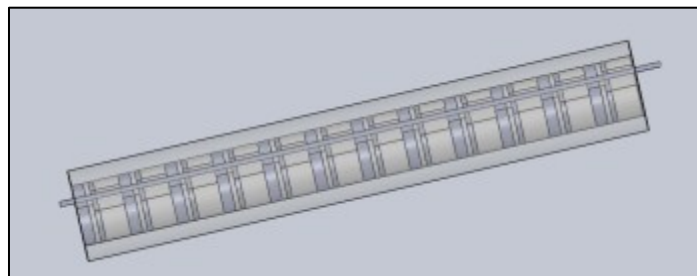


**Figure 17: Original 12-Electrode Pump Section**

In the image above, the electrodes are housed within a single insulator tube. The unique design of these electrodes, which was shown in one of the previous sub-sections, relies on the tight fit of this insulator tube in order to force the busline wires (one of which is shown on the previous page as well) into contact with the electrodes. One busline is therefore shared between all the high-voltage electrodes and another is shared between all the ground electrodes.

This design evolved as did the design for the hard, metal housing for the entire pump device. The initial housing idea had six pump sections side by side in flat cartridge. The issue with this design was that the tube pipes available in the lab for our use could not be bent at a very sharp angle. Since the tubes' minimum bending radius was far too large the pump sections would have to be spaced out such that the cartridge would need to be about a meter in length – equally undesirable as the linear, single section design.

Therefore, the design evolved to a series of staggered pump housings comprised of multiple housing “cartridge” pieces, each containing three pump sections, which would be connected via tubes in series. The first such design tried to address possible leaking issues by incorporating endcaps that would be press-fit onto central housing pieces, shown below:

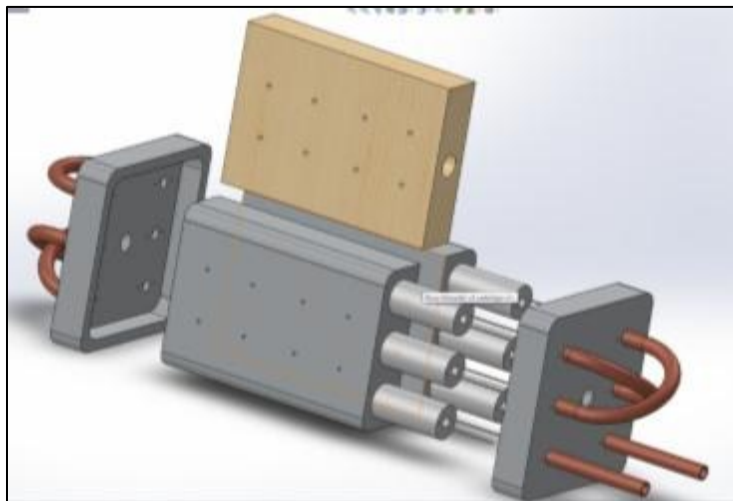


**Figure 18: Housing Design Incorporating Endcaps**

This design attempted to occupy the least amount of space and use as little material as possible while still offering a thick enough metal surrounding for each pump section to make sure no breach occurs during operation. To save on manufacturing costs and weight, the space between the housing pieces was eliminated and replaced with wood. Initially, it was thought that the endcaps could be pressed together to seal both sides of the housing using a large center bolt. The center hole for this bolt can be seen in the image on the previous page, going through the wooden block and both endcaps. Another feature of this initial design was that the buslines actually went out through the endcap pieces (the image shows small holes for them on each side of the holes for the tubes), such that the high-voltage and ground connections would need to be connected to each pump section separately.

The endcap idea was later scrapped since it was determined that even such a press-fit would not offer enough of a seal to avoid leaks in the system. The large amounts of contact surface area would distribute the pressing force and would therefore allow for many small leaks at the edges. In all future designs, bushings and pipe fittings were used instead to connect the tubes to the housing pieces and avoid leaks.

The final issue with this design was that the 1.125" diameter, 12-electrode pump sections required an 8" long hole to be drilled into each housing piece – too long based on manufacturing standards for the ratio between the hole diameter and the hole length. Therefore, the pump section size was reduced to 8 electrodes for an overall hole length of 6", which was more feasible to manufacture. This resulted in the need to add another housing piece, for a total of three housing cartridge pieces each containing three pump sections.

## Final Design

As previously mentioned the final design was comprised of three housing cartridges, containing nine pump sections, with two wooden spacers in between them. To correctly connect all the pumping sections in series in this configuration, the following schematic was implemented. The “within face” portions represent the connections between the housing cartridges on either side of the pump assembly. The “entry” would therefore be the overall device inlet and the “exit” would be the outlet.

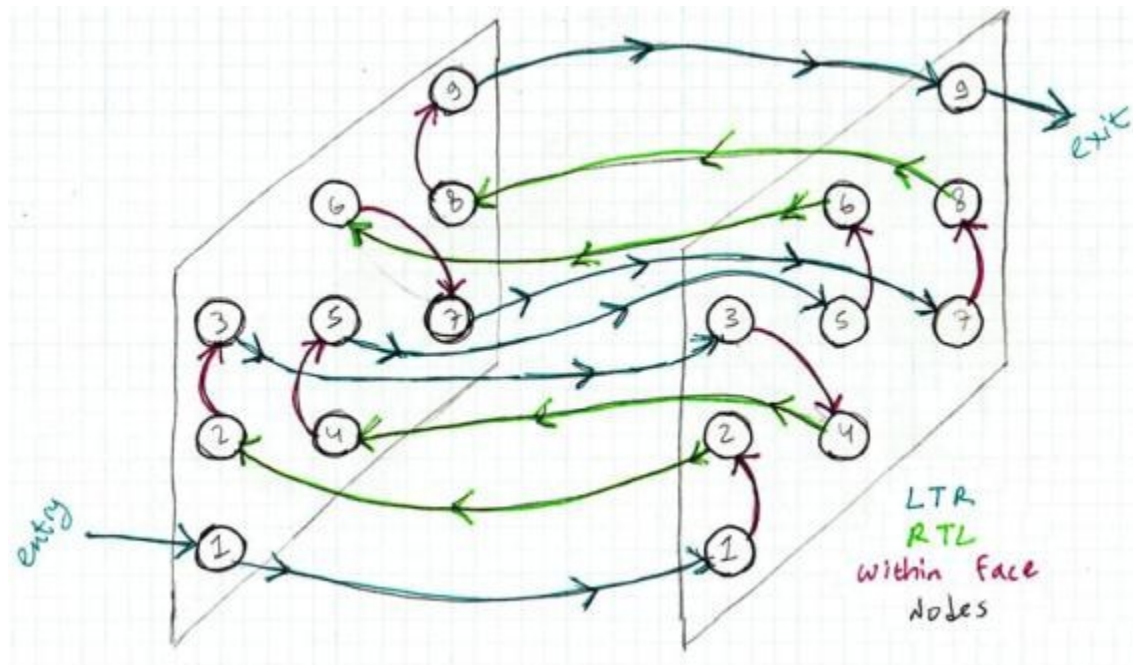


**Figure 19: Tube Paths between the Nine Pump Sections**

Along with the shortened pump section design, each pump section’s insulator housing was changed as well to offer more protection and a better enclosure for the electrodes. In this new design, the insulator tube containing the electrodes is divided into three sections that are easy to manufacture. The two endcap pieces of this housing have holes that allow the 1/16” gage buslines to protrude out on either side. The busline ends are threaded and small nuts keep the entire housing fitted together snugly. This design can be seen on the following page.

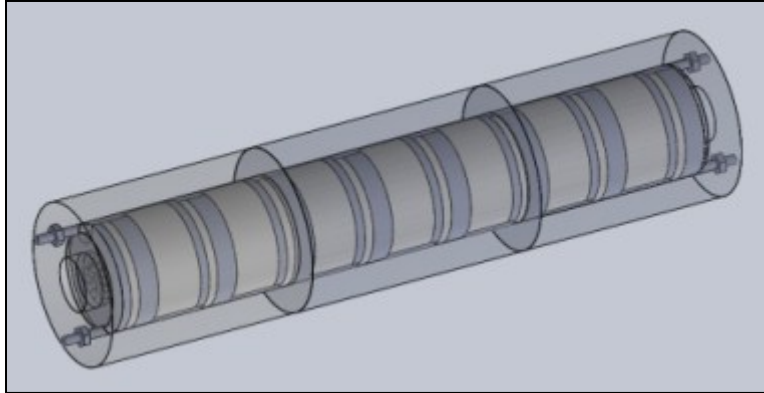


**Figure 20: Final Pump Section Design**

The following images shows the design for a single metal cartridge, with a pump section inserted into one of its holes:

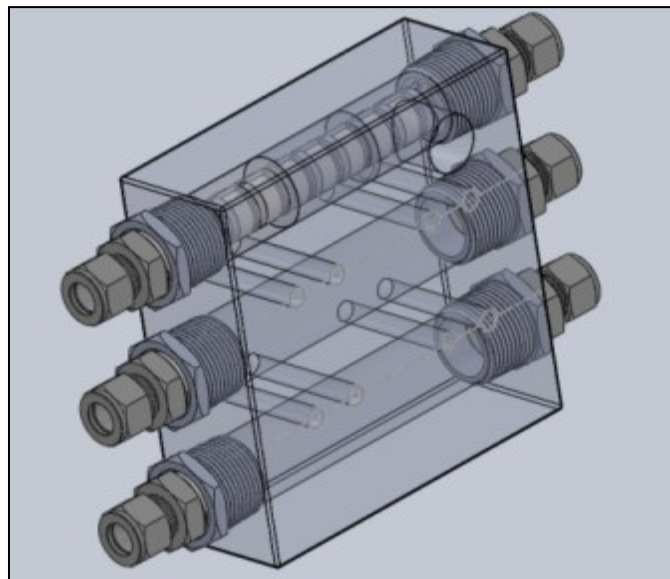


**Figure 21: Multi Pump Section Housing Cartridge**

As can be seen in the above image, the pump section is fully enclosed within this housing cartridge and the buslines do not protrude out from it. Therefore, this design includes both a high-voltage plug, at one end of the assembly and a ground plug at the other, with wires going through the tubes connecting the pump sections together and to each plug. The holes for the high voltage and ground plugs can be seen on the top right corner of the image above.

The final overall design can be seen below:

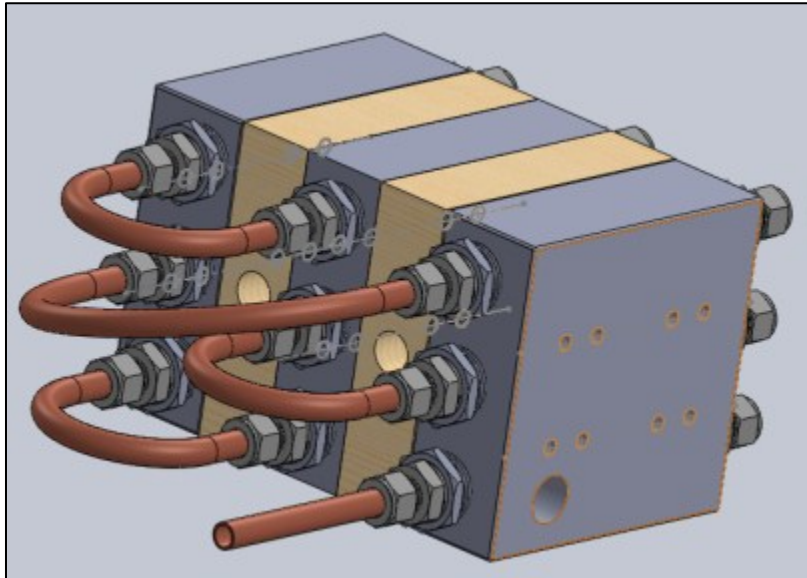


**Figure 22: Final Pumping Device Design**

This image shows the hole for the ground/high-voltage plugs more easily. Note that the center cartridge does not have such a hole, since only one ground plug and only one high-voltage plug are required. This image also shows how the tubes would connect the pumps in series from one side of the device – the back side being almost a mirror image of the front. In this design, adding or removing cartridges and even pump sections from individual cartridges can be achieved relatively easily, as only the tube connections would need to change. The holes on the side of this design can be used to insert long bolts through the entire assembly to press fit it all together and maintain the device as a single unit. This final design was born out of the many unforeseen manufacturing limitations, but still fulfills the design goals described in the overview of this section.

## Experiment Design

Designing the experiments for the proof of concept device described in the previous subsection was a relatively easy task. The choice of working fluid meant that temperature did not need to be monitored, since the boiling point of HFE-7600 is very high. In addition, although one of the goals of this project was to study the flow rate generated by the proof of concept pumping device, it was an optional goal and was discarded as the end of the project drew near. Therefore, only a static pressure differential was of interest and only a single pressure transducer was needed to measure it. The other quantities that needed to be measured to ensure that the pump was working were the input voltage – to ensure that the correct voltage was being applied at each step of the experiment – and current consumption – to ensure that no sparking occurred, which is characterized by sudden spikes in current levels.

The following image shows the front panel of the LabVIEW program that was implemented for the experimental portion of this project. The program takes 10 samples per second of each of the quantities and records them into a file in a format that can be easily loaded into Matlab or other computational software:

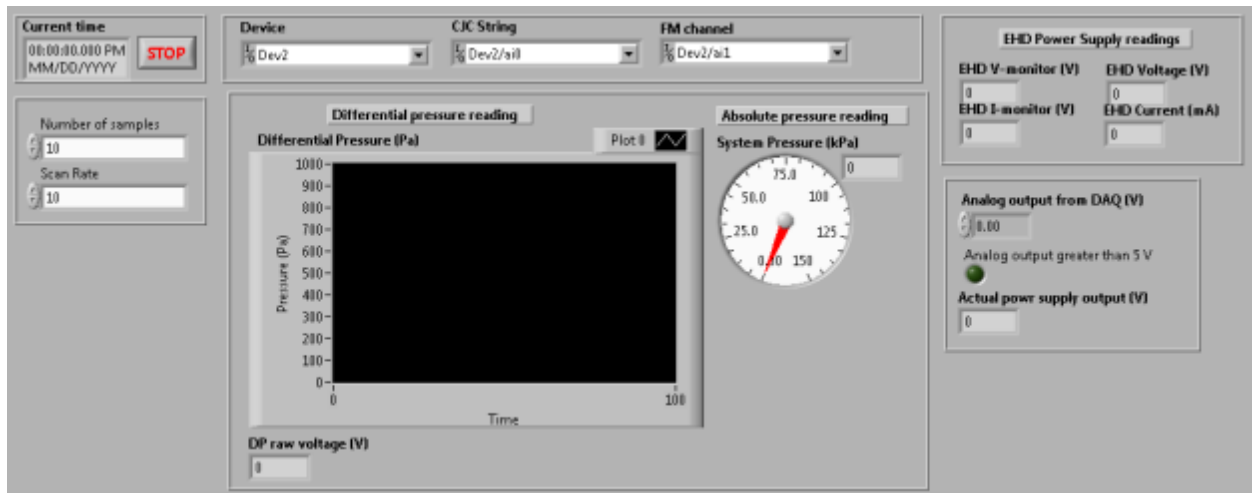


Figure 23: LabVIEW Front Panel

The experimental process was therefore designed to follow these steps:

- Assembly of a single pump section in a single housing cartridge
- Testing pressure generation for a single pump section
  - HFE-7600 as the primary working fluid
  - R-123 as the secondary working fluid if time permitted
- Assembly and testing the remaining two pump sections for a single housing cartridge, one by one, to observe the additive effects of each one
- Assembly and testing of the remaining complete cartridges and observing the additive effects of entire cartridges to the final pressure generation

## **Material Selection**

The selection of materials to construct the pumping device from had to carefully checked against the working fluid to be used in the pump. Since many dielectric fluids are unsafe to use and can have adverse reactions with a wide range of materials, it was imperative to consult the safety manual for the HFE-7600 fluid, and for the R-123 fluid as well if time permitted, before deciding on materials. Luckily, both HFE-7600 and R-123 are safe to use with a large variety of materials, including many metals, most plastics and silicone glue.

The only option of material for the high-voltage electrodes was stainless steel, as that is what the manufacture used to construct them. To make sure that there would be no issue with the electric conductivity between the high-voltage electrodes and their housing disc due to having them be made from different materials, it was decided to have the housing disc made from stainless steel as well. Similarly, the buslines were also made out of stainless steel. However, this

selection was more due to the availability of wire of the appropriate gage in the lab than due to the electrical connections.

For all the insulating spacers and the insulator pump section housing, PTFE (generic version of Teflon) was selected because it is an excellent electrical insulator that does not deform easily in the piece sizes we needed. It is also easier to machine than many other plastics.

All tubing and pipe fittings were provided from the lab, in copper and brass. Lastly, aluminum was selected both for the ground electrodes and for the cartridge housing pieces. Not only was aluminum the lightest choice for metal that fit within our operational budget for the cartridge pieces, it is also the easiest metal to machine at the Washburn Machine Shop at no additional cost.

## **Manufacturing Process**

The manufacturing process for the final design turned out to be more complex than originally thought. Since all of the design work was done in SolidWorks it was easy to import the finished models into Esprit – the manufacturing software used at the Washburn Machine Shop – in order to program the manufacturing process directly onto the model geometry. However, figuring out which process and which tools to use for which geometry, as well as what speeds and feed rates to use for each tool, proved to be a daunting task. The staff at the Washburn Machine Shop was therefore instrumental in bringing our designs to life.

Both the ground electrodes and the wide spacers were made out of long bars of material (aluminum and PTFE respectively) in a lathe using LiveTooling. Normally in a lathe, the workpiece bar is made to spin and the tools remain stationary relatively to it, thus achieving the

same relative velocities and feed rates as one would if the bar was stationary and the tool was spinning. LiveTools, however, are able to move on their own as well, allowing them to machine more complex geometries, such as the curved cutouts on the top and bottom of the electrode and spacer pieces. This relatively complex process was handled primarily by the experienced Washburn Shop staff.

The PTFE pump section housings were first cut out of a long bar in a lathe and then were machined on either side in a CNC machine. Since the CNC machine is not normally equipped to clamp down on round pieces, especially ones that are made of a plastic that is much more pliable than metal, a special “soft jaw” clamp had to be machined to hold the pieces, shown below:

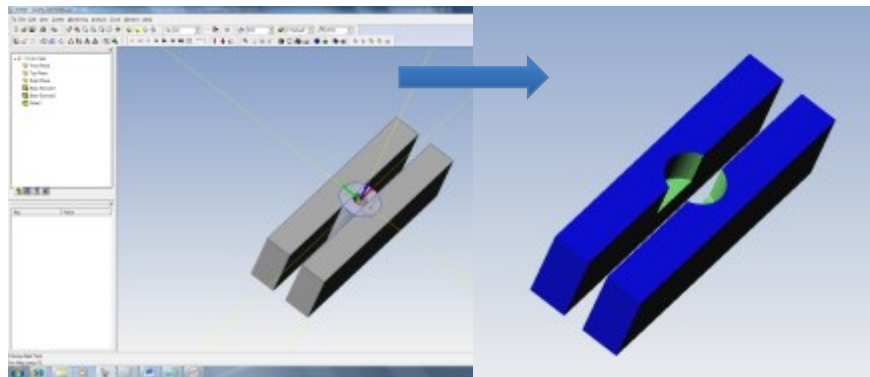


**Figure 24: Soft Jaw Clamp**

To make sure that the program for machining these PTFE pieces worked correctly, test pieces were first machined out of aluminum or brass. Initially, several corrections needed to be made both to the program and on the CNC machine itself, in order to make precise parts.

Machining these PTFE pieces turned out to be an easy and accurate process that did not take very long, making these pieces the easiest to manufacture overall. As an example, the program used to make the top of an endcap piece is shown, along with the metal prototypes, on the following page.

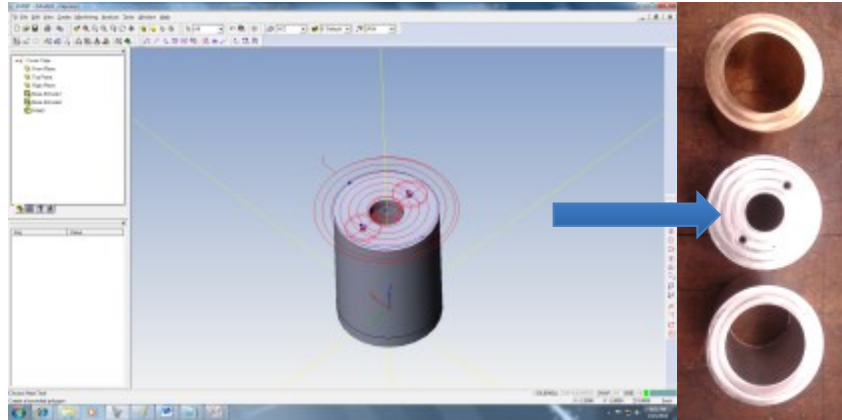


**Figure 25: Example PTFE Endcap Test Piece Manufacturing**

The cartridge housing pieces were manufactured out of solid blocks of aluminum in a CNC machine. First, each block had to be cut down to the final dimensions of the cartridge, ensuring that every side of the cartridge would be perfectly straight and smooth. Then, the 6” long holes for the pump sections had to be drilled as 3” holes from each end of the cartridge piece. To make this difficult process easier, the locations of the long holes’ centers were pre-tapped lightly by a drill in the CNC machine, ensuring that the hold locations are accurate. Then, an 11/16” manual drill press was used to make an initial clearance path all the way through the cartridge. This too had to be done 3” from each side of the cartridge, but alignment was not important at this step. With the clearance holes in place, a flat endmill was set to plunge into the clearance hole incrementally and carve out the final shape of the hole, 3” from each side. Once this was done, the holes on the side of the cartridge were drilled and the hole for the ground plug was endmilled as well.

Once the cartridge pieces were finished, the holes in them had to be tapped using a 1” NPT tapered tap for the pump section holes and a 3/4” NPT taper tap for the ground plug hole. Since the Washburn Machine Shop did not have a tap handle for the larger tap, one had to be made from scratch.

The images below show the different steps for manufacturing the cartridge pieces in the CNC machine:

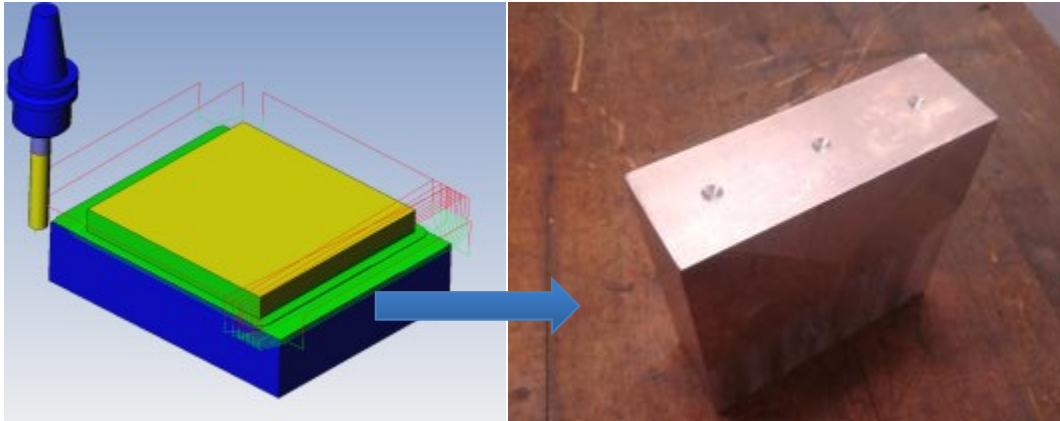


**Figure 26: Carving Out & Pre-Tapping the Cartridge**

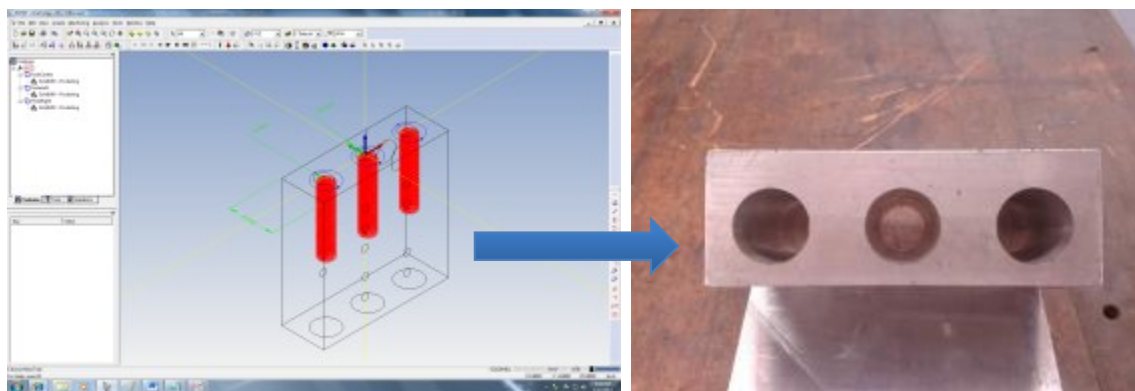


**Figure 27: Drilling Long Holes from Each Side of the Cartridge**

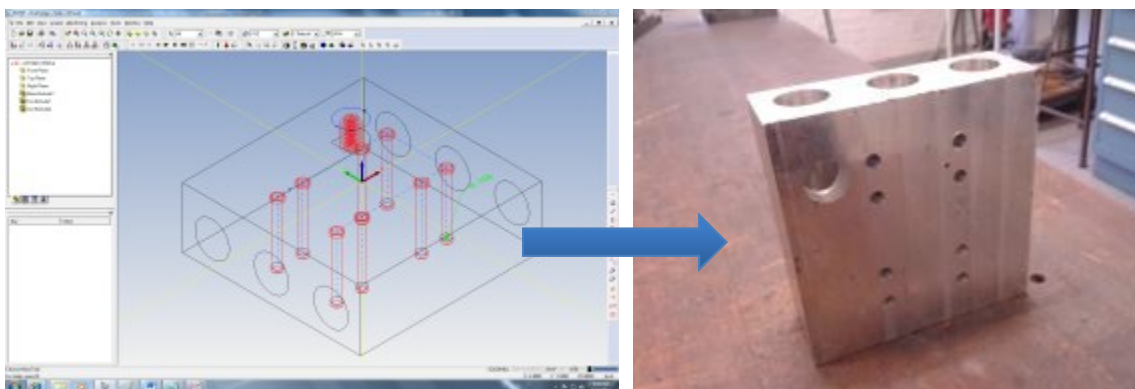


**Figure 28: Drilling the Side Holes in the Cartridge**

Since the Washburn Shop did not have the facilities that could manufacture the stainless steel housings for the permeable porous electrodes, those were manufactured at Howard Products Sheet Metal in Worcester. Finally, the thin spacers were laser cut out of a thin PTFE sheet.

Both the aluminum ground electrodes and the stainless steel housings for the permeable porous electrodes were put through a deburring tool in order to try to grind down any sharp edges they might have since sharp edges can cause ion injection, like in ion-drag pumping, which counteracts the conduction effect and degrades the electrodes.

## **Assembly Process**

The first assembly process was the insertion of the stainless steel porous electrodes into their stainless steel housing. The issue here was securing the permeable porous electrodes to the ring housing. A couple of tests were conducted with the extras that were ordered and it was found to be exceedingly difficult to solder the parts together without having the solder absorbed into the porous center or having it leave sharp edges that cannot be ground down. The next option was to weld the parts together using a spot welder and after many trial runs an acceptable process for producing the final high voltage electrodes was established and executed.

After this obstacle, the first pump section needed to be assembled from the electrodes and insulator housings. This proved to be more difficult than initially thought due to the many small pieces that comprised a section and the difficulty in ensuring that everything had the correct placement and alignment and was firmly pressed together to preserve the correct spacing between the electrodes. For this purpose, a rig was created by bisecting a copper tube in two to create two cradles. The cradle was stabilized using spare, heavy brass pieces and small, round

brass pieces were used to press the electrodes together in the cradle. The image below shows the cradle assembly and how electrodes could be fitted into it, with a busline on top:

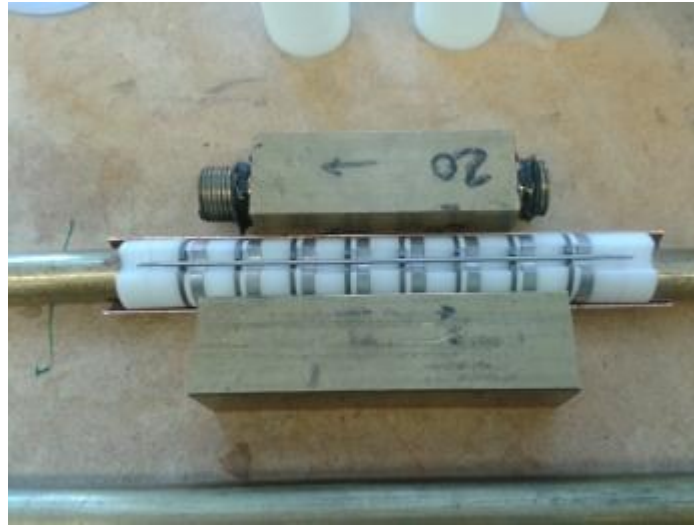


**Figure 29: Pump Section Assembly Using a Cradle**

A big issue that quickly came to light was maintaining the good electric contact between the electrodes and their buslines. It turned out that the press fit into the housing did not yield as good a result as expected, even when the buslines were glued down to the electrodes using silicon glue. Therefore, it was decided to use solder on both the high voltage electrodes and the ground electrodes to try and make the contact better. However, since the ring ground electrodes were manufactured in the WPI Machine Shops out of aluminum instead of steel, the solder could not stick to them. However, since silicon glue was being applied to the pump anyway, it was used to ensure contact between the solder and the ground electrodes. It also served to cover any sharp edges that the solder might have.

After applying the silicon glue on either end of the pump, the assembly had to be left for a minimum of 24 hours to allow the silicon to completely dry. During this time, pressure was applied to the pump assembly to ensure that the silicon glue would fill all the cavities present, to

provide for better structural integrity as well as good electrical contact with the solder and the electrodes. The image below shows how a weight was placed on top of the compressed pump section, once silicon has been applied:



**Figure 30: Weighing Down a Pump Section to Ensure Contact with the Busline**

Overall, putting the pump sections together turned out to be one of the more complex tasks of this Major Qualifying Project. So much so, that a guide had to be drawn up for making them so that no step in the long process would be skipped or forgotten. This guide can be found in the appendix section of this report.

The next step was pushing the section into the PTFE housing shown below:

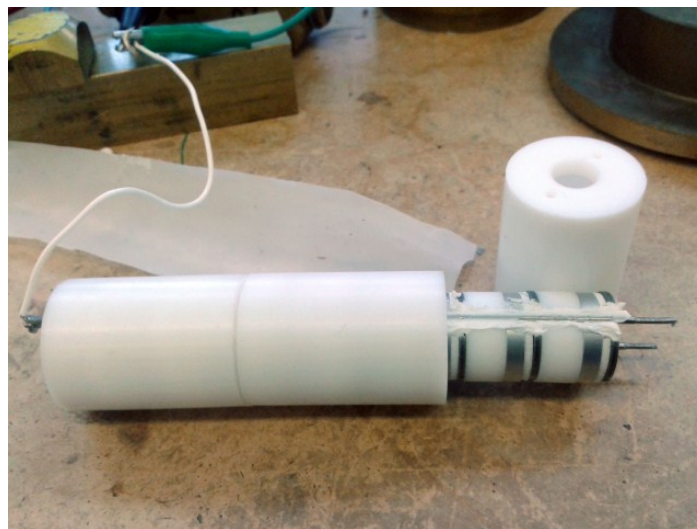


**Figure 31: Assembled Pump Section Inserted into Insulator Housing**

The bus lines fit easily into the holes in the endcaps and had washers and nuts placed on them to fir the housing together. This step concluded the assembly of a single pump section, which could now be inserted into the cartridge piece for testing.

An issue encountered while attempting to connect the ground plug at the side of the aluminum housing was the tight dimensions that prevented the wired from being passed alongside the pump section's housing so it could be connected to the ground busline. Therefore, a slit on the inner corner had to be made to allow free passage of the wire. The slit is shown below and was far in enough so that it did not cause any issues with leaks or proper fastening of the ground plug or the bushings and fittings on the end of the cartridge:



**Figure 32: Pass Through Slit for Ground Wire**

A pump section could then be inserted into the bottom (pre-cleaned) channel in the cartridge and fitted with the ground wire from the adjacent ground plug, as well as wires to the high-voltage connection. Bushings could then be screwed into either end of the cartridge channel so that the pump section could be connected to the rest of the assembly.

For the first experimental case, only one pump section needed to be used, so an experimental setup was first assembled around using just the one section. Since the high-voltage

plug was on a separate cartridge, it was decided to connect the high voltage to an external point in the assembly and simply run a wire to the high-voltage busline through the tubes. The ground plug could remain as is and would be used to ground the entire assembly. The remainder of the setup was put together from pipe fittings that needed to be cleaned and fitted with Teflon tape to prevent leaks, and from copper tubing that needed to be bent to the appropriate shapes.

The original experimental setup assumed that the pump could be evacuated by pulling a vacuum from one end and then filled from the same end. Therefore the setup was relatively simple, as shown below:

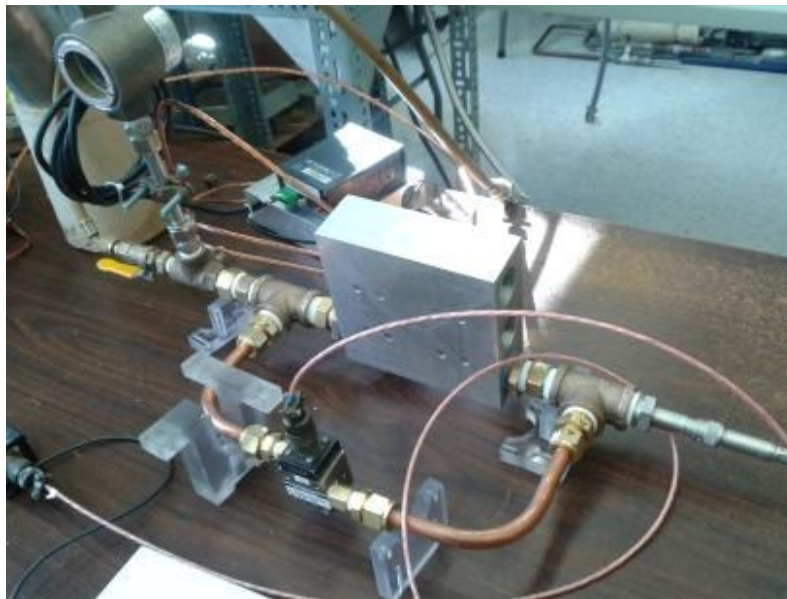


**Figure 33: Initial Experimental Setup**

The high-voltage connection can be seen on the right side of the image. The pressure transducer is connected in a way that allows it to measure the differential pressure across the pump. On the left side of the image a valve for pulling a vacuum can be seen. A sight glass is fitted to the top of this assembly to ensure that the working fluid's vapor phase would have a

space to expand to and to allow for a visual confirmation of the pump being filled. The fill port for the pump is at the top of the sight glass, on the same side of the pump as the vacuum port.

Due to lack of experience and the pliability of copper, the copper tubing portions had to be re-measured, cut and assembled several times as they would either fit poorly such that the assembly could not hold pressure and would leak, or such that the tubes would bend permanently when put together without perfect alignment. In addition, since the cartridge was manufactured at WPI, it did not follow the strict tolerance of commercial pipes and therefore leak-lock had to be applied to all of its holes immediately before any bushings or plugs could be fitted in and then allowed to dry together overnight.

After the leak-lock was allowed to dry and the pump was completely put together, it was pressurized in order to test for leaks. Leaks were tested both with a water bath and with soap. If bubbles were observed in either case on any connection it was tightened. If the pump was able to lose less than 1 psi of pressure in half an hour, it was deemed experiment-worthy and a vacuum could then be pulled from it. Once a vacuum was pulled, the pump could be filled. Once filled, the resistivity of the fluid was checked and, if it was under 10 MOhms, the pump was ready to run, if not the pump was shaken and allowed to fill more.

After the first trial runs of this experimental setup, it was determined that the pump was not filling being filled completely with the working fluid, despite the vacuum. Having empty space within the pump meant that it could not run at anywhere near the applied voltages needed for the experiment, since it would begin to spark too soon. An attempt at creating a bypass to allow the fluid to go around the pump and therefore fill it from both ends was made, which was helpful but did not completely solve the issue.

In the end, the fill port for the pump device was moved to the opposite end of the cartridge from the vacuume port and the bypass was removed. This forced the working fluid to fill the pump before arriving at the other side and filling the sight glass.

Lastly, the high voltage connection and ground plug had to be connected to the power supply and a DAQ board box had to be wired and set up to work with both the computer and the power supply. This setup took after a previous project that was in the lab and required careful wiring to the correct inputs and outputs of the high voltage power supply. The setup behind the high voltage power supply is shown below and further wiring was done within the DAQ box.

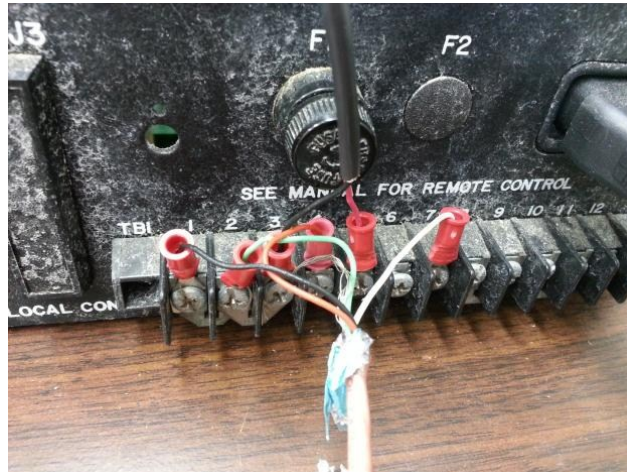


**Figure 34: Power Supply Wiring**

## **Final Experimental Setup**

A diagram of the final experimental setup is shown on the following page. In this diagram, the new fill port can be seen on the left, on the opposite side of the pump from the vacuum port on the right. During operation, the valve to the sight glass would be closed, closing off the pump loop in order for us to observe the static pressure generation case.

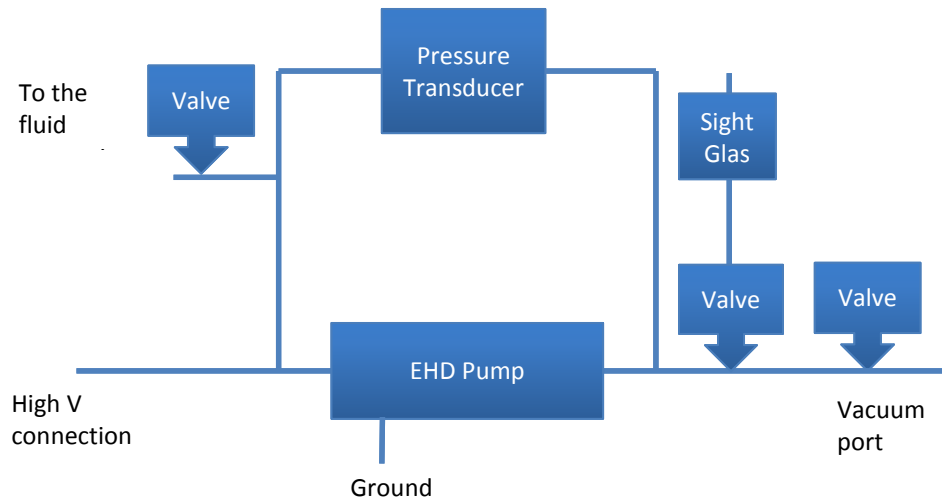


**Figure 35: Experimental Setup Design Diagram**

The final assembly is shown below:



**Figure 36: Final Experimental Setup**

This image shows the fluid tank above the entire pump in an IV fashion that uses gravity to help fill the pump. The issue with this design was the possibility that the fluid would rush into the pump and the resulting pressure of the fluid on the porous electrodes could pop them out of their housing and cause a short in the pump. Therefore the fluid had to be carefully let in by only partially opening the two valves into the pump. The first attempt at filling the pump failed and when disassembled it was determined that one of the permeable porous electrodes had come loose from its housing. This assembly yielded the best experimental results, but is still not fully perfect as the pump still needs to settle over time and shaken slightly for the fluid to completely fill the pump.

Due to time constraints, no further pump sections were added to this assembly. The results obtained using this single-section setup can be found in the following section.

# Chapter 5: Results

## Overview

This section shows the results of the data that was collected during the final test run of the single-section pump described in the previous section.

## Pressure Generation

The results of the final test that was run on the final pump device are shown below. The generated pressure differential and the applied voltage are plotted as a function of time. The applied voltage was increased by 500 volts every 60 seconds:

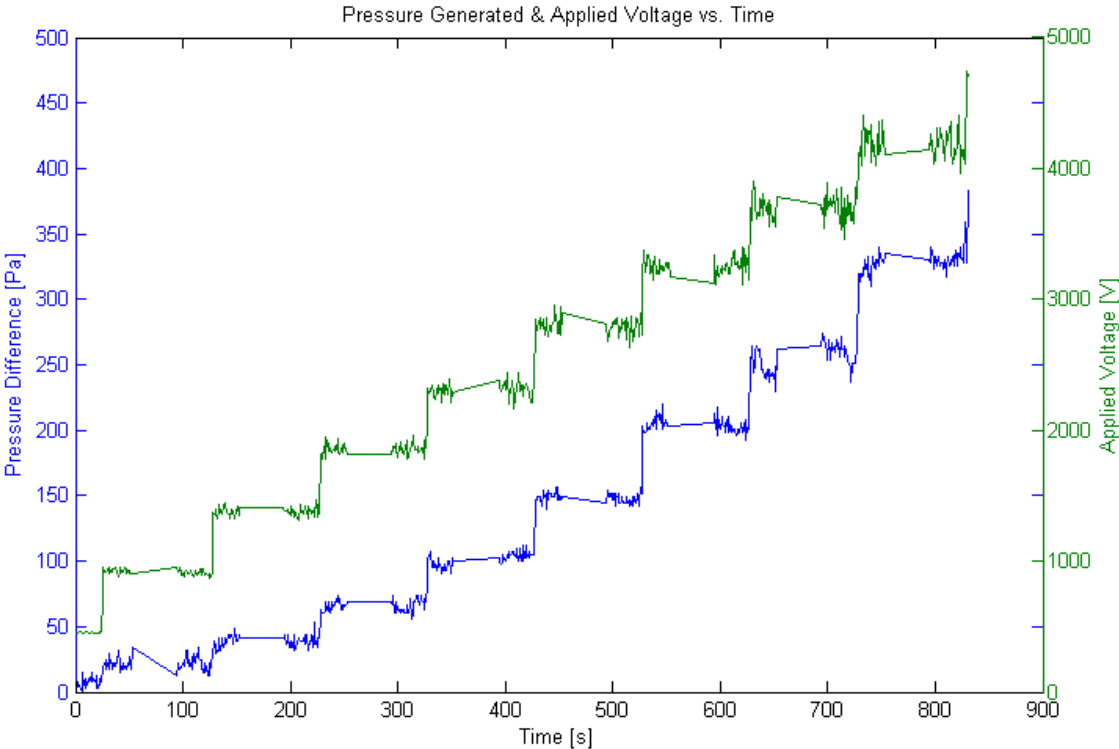
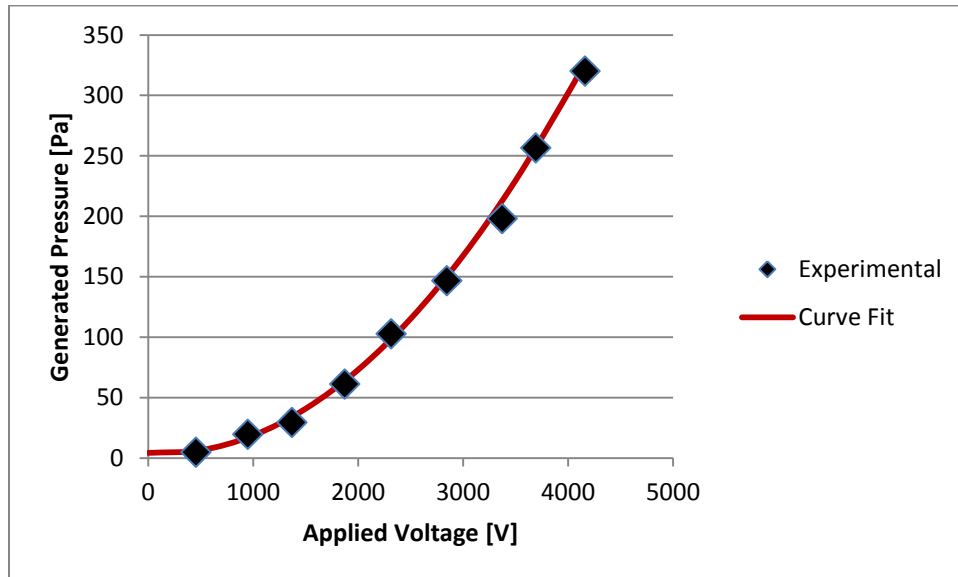
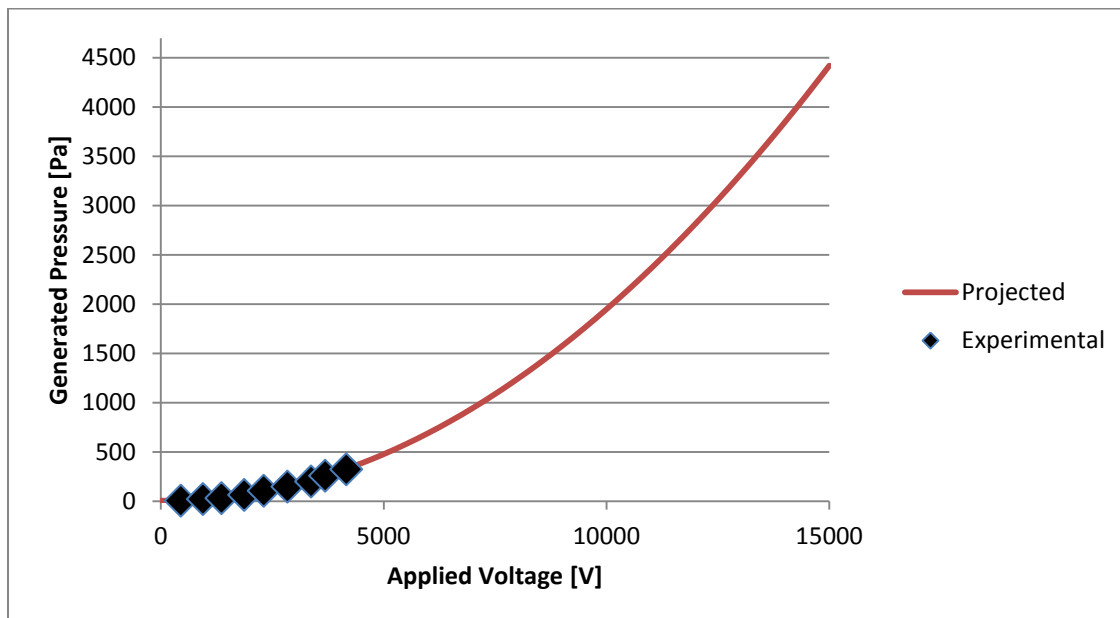


Figure 37: Final Test Results

The images below show the extracted plot of the generated pressure differential versus the applied voltage, as well as an overall performance estimation plot based on a polynomial curve fit applied to the experimental data:



**Figure 38: Generated Pressure vs. Applied Voltage**



**Figure 39: Projected Performance Based on Experimental Data Curve Fit**

# Power Consumption

The image below shows the current consumption versus the applied voltage during the final run of the pump device. The error bars denote the standard deviation of the measurement:

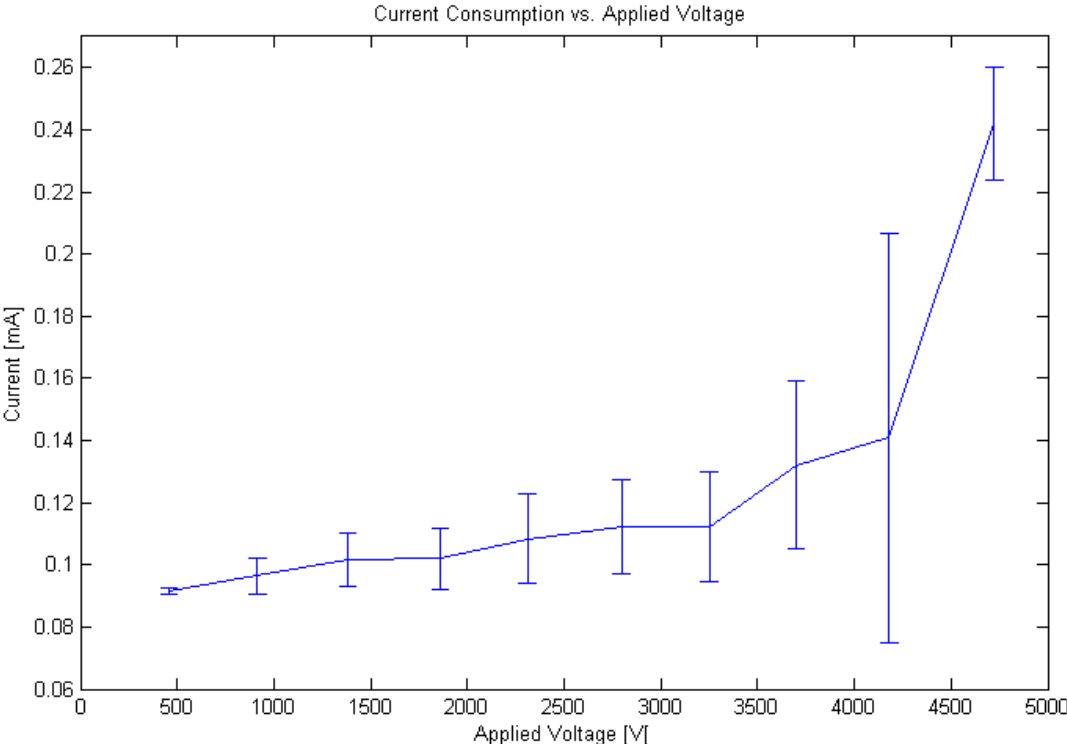


**Figure 40: Current Usage during Final Test Run**

## **Chapter 6: Discussion**

### **Overview**

Manufacturing and running the pump turned out to be the most challenging part of the Major Qualifying Project. Between manufacturing constraints, leaks in the loop, air trapped in the pump, electrodes being dislodged, and filling issues, there were many challenges that needed to be addressed and resolved to have a successful run and acquire meaningful data.

However, the data that was collected was promising and, if the problems could be corrected, projections show that the one pump section should be able to generate the amount of pressure expected of it. This section offers a discussion of the most meaningful results as well as an overview of the challenges encountered and future work that still needs to be done.

### **Major Results**

The major results of this project were collected after several different runs of the EHD pump, each with a different iteration of the pump section with the performance increasing drastically between each improved pump section. The final section tested constituted the most major improvement due to the soldered connections. During this final test, the pump was able to handle up to 4kV before experiencing sparking due to filling issues. The sparking effects can be seen in Figure 40, which shows the current consumption of the pump versus the applied voltage, with the standard deviation on each measurement. At 4kV, the standard deviation is significantly higher as the current was rising and falling wildly. In general, the current consumption for this pump was uncharacteristically high for an EHD conduction pump, leading to the belief that ion

injection was occurring within the pump, which was likely decreasing the overall pressure generation effect and enabling sparking to occur.

At 4kV, the maximum generated pressure differential was 360 Pa. As can be seen in Figure 38, the plot of the generated pressure differential versus the applied voltage follows a steep exponential gain. Figure 39 shows a continued projection of this exponential gain to the highest applied voltage that was safe to apply, based on the experiment design and previous runs. According to this projection, the pump section should be able to generate 4-4.5 kPa of pressure under the maximum applied voltage. This is precisely the level of pressure needed in order to have a total pressure of 0.3-0.4 atmospheres, since the pressure from all nine sections would add up nearly linearly. These final results of this proof of concept show that with further testing and continued improvements to both the pump itself and the experiment setup, it would be very possible to achieve the pressure generation desired for this project.

## **Encountered Issues**

Like most scientific experiments, this project encountered a multitude of issues, from manufacturing and assembly to problems with electrical connections, before it was completed - some of which were resolved but some that still need additional work.

Many of the issues that were resolved were with the manufacturing phase of the project, since items that seemed like they would be easy to manufacture turned out to be complex, causing unforeseen delays and additional costs. In addition, although the Washburn Shop's equipment is top notch, it is not a high-accuracy manufacturing facility. Therefore the tolerances on the manufactured parts varied, causing alignment and fit issues with the final parts. Luckily,

quick redesigns, corrections of the manufacturing instructions and the occasional use of epoxy glue were able to correct the vast majority of these issues over time.

However, even after manufacturing, what had been originally thought of as a simple design that could be easily assembled turned into a complicated task with many steps that took a long time to perform. Anything involving silicon and leak-lock, in particular, required the pump to be left alone for a minimum of 24 hours. This means that every time the pump had to be reassembled and a new pump section had to be made, testing was delayed by a work week. This issue is not necessarily problematic on its own, but the time delays were unforeseen and made the testing phase of the project less comprehensive than it otherwise should have been.

The biggest yet not entirely resolved issues were discovered during the testing phase of the project. Unfortunately, virtually all issues present during the pump's operation result in the same symptoms – sparking – which makes it difficult to pin-point the exact causes for the system's failure. Sparking can occur due to the presence of small metal particles, air or a vapor phase of the fluid in the area affected by the electrodes' electric field. Any of these can cause the current draw to increase dramatically and create a spark that begins to break down the working fluid. When filling the pump, if the pump was not completely filled with the liquid, air bubbles would get trapped inside and increase the measured resistivity between the high-voltage connection and the grounded assembly. Another likely reason for the sparking is the fact that there were some sharp edges within the pump, like the edges of the high voltage and ground electrodes, from which ion injection can occur. For the final pump section that was tested, all efforts were made to remove any air and fill every empty space within the pump and the pump was filled with fresh fluid devoid of any contaminants. Sandpaper was also used to smooth some of the sharp corners and edges of the electrodes in hopes that it would eliminate the sparking.

Other issues that arose while assembling the setup were leaks within the loop. If one of the connectors or tubes was not completely sealed, it allowed air to enter the system. The leaks would then make it so a deep enough vacuum could not be pulled and air would constantly seep into the pump during operation, making the pump unusable. To resolve this, extensive leak testing had to be performed each time the loop was reassembled, as described in the assembly process. Initially, the pump had very large leaks, primarily due to an issue with the grounding plug. In the end, the grounding plug had to be mounted on an extension that was epoxied to the cartridge, which eliminated the leak and had the added advantage of making the pump more reliable, since the original ground plug had been impinging on the pump section, damaging the insulator housing and possibly affecting the busline connectivity.

Lastly, keeping the high voltage electrodes in place inside their housing discs was another important issue in this project. As mentioned previously, at first the high voltage electrodes were to be soldered to their housing discs but the only means available to do so were crude and the result had sharp edges and protrusions that prevented the electrodes from fitting alongside the rest of the pump pieces. Spot welding was therefore used, which did add any sharp edges, but had the adverse effect of melting the edges of the electrodes, making their active surface area smaller and providing a less than ideal attachment. Because the electrodes were not fully secure within their housing, when the pump was tested some of them became dislodged and caused shorts. This issue could not be fully resolved and only very careful handling of the pump sections allowed for the promising results obtained during the testing phase.

## Future Work

In order for the full design of the nine-section pumping device to become fully operational, additional work needs to be done both on the individual pump sections and on the overall testing assembly. First and foremost, any and all issues that cause sparking must be resolved to allow the device to handle an applied voltage of 15 kV. This includes making sure the high voltage electrodes stay in place either by finding a better way to attach them to their housing discs while maintaining the electrical contact between the two, or by redesigning these electrodes and how they connect to the buslines. In addition, a filling process has to be developed such that the pump would be filled entirely in a reliable and repeatable fashion, without any air or vapor phase trapped within it. Lastly, investigating the reason for the ion injection and figuring out an alternative to solder for maintaining the integrity of the electrical connections would be greatly beneficial as well.

If these improvements are implemented and testing is to continue, the first goal would be to have a successful run with one pump within the housing at the maximum applied voltage. After that, the remaining pumps could be added to the housing and loop until all nine pumps are connected, as described by the original experiment design.

Overall, the issues encountered during this project can all be resolved given additional time and effort. The work done thus far has provided a good basis to build from and certainly shows that the final goal can be achieved.

## **Conclusion**

EHD conduction pumping technology shows great promise as a means for hydraulic pressure generation. Although the final planned goal of this Major Qualifying Project was not fully achieved due to time constraints, a proof of concept device capable of generating pressure was successfully realized and tested. In addition, the pressure curve generated thus far with the device proves that generating between 0.3 atmospheres and 0.5 atmospheres of differential pressure should be possible at the maximum designed voltage input, with the full, compact nine-sectioned device described in this report. These results confirm the original numerical estimations performed during the analysis phase of this project, within the safety factor specified. Thus, even though further work would be required to complete the full device, the concept behind it has been proven to be sound.

## References

- Abe, R., Takemura, K., Edamura, K., & Yokota, S. (2006). Concept of a Micro Finger Using Electro-Conjugate Fluid and Fabrication of a Large Model Prototype. *Elsevier Sensors and Actuators*.
- American Society of Heating. (2005). Refrigerants. In *ASHRAE Handbook - Fundamentals*. Refrigeration and Air-Conditioning Engineers, Inc.
- Chen, C., Selvarasah, S., Chao, S., Khanicheh, A., Mvroidis, C., & Dokmeci, M. R. (2007). An Electrohydrodynamic Micropump for On-Chip Fluid Pumping on Flexible Parylene Substrate. *IEEE International Conference on Nano/Micro Engineered and Molecular Systems*. Bangkok, Thailand: IEEE.
- De Volder, M., & Reynaerts, D. (2010). Pneumatic and Hydraulic Microactuators: A Review. *Journal of Micromechanics and Microengineering*, Vol. 20.
- Feng, Y., & Seyed-Yagoobi, J. (2004). Control of Liquid Flow Distribution Utilizing EHD Conduction Pumping Mechanism. *39th IAS Annual Meeting, Industry Applications Conference* (p. Vol. 4). Seattle, WA: IEEE.
- Feng, Y., & Seyed-Yagoobi, J. (2004). Understanding of Electrohydrodynamic Conduction Pumping Phenomenon. *Physics of Fluids - American Institute of Physics*, Vol. 16.
- Gilbertson, R. G., & Busch, J. D. (1996). A Survey of Micro-Actuator Technologies for Future Spacecraft Missions. *The Journal of the British Interplanetary Society*, Vol. 49.
- Jeong, O. C., Park, S. W., Yang, S. S., & Pak, J. J. (2005). Fabrication of a Peristaltic PDMS Micropump. *Elsevier*.
- Jeong, S. I., & Seyed-Yagoobi, J. (2004). Innovative Electrode Designs for Electrohydrodynamic Conduction Pumping. *Industry Applications, IEEE Transactions on*, Vol.40.
- Jeong, S., & Seyed-Yagoobi, J. (2002). Experimental Study of Electrohydrodynamic Pumping Through Conduction Phenomenon. *Elsevier, Journal of Electrostatics*, Vol. 56.
- Kang, H., Lee, I. H., & Cho, D. (2006). Development of a Micro-Bellows Actuator Using Micro-Stereolithography Technology. *Elsevier Microelectronic Engineering*, Vol. 83.
- Kashani, R., Kang, S., & Hallinan, K. (2000). Micro-Scale Electrohydrodynamic Pumped High Performance Actuation. *Journal of Intelligent Material Systems and Structures*, Vol. 11.
- Kazemi, P. Z., Selvaganapathy, P. R., & Ching, C. Y. (2009). Effect of Electrode Asymmetry on Performance of Electrohydrodynamic Micropumps. *Journal of Microelectromechanical Systems*, Vol. 18.

- Linag, S., Xu, J., Weng, L., Zhang, L., Guo, X., & Zhang, X. (2007). Biologically Inspired Path-Controlled Linear Locomotion of Polymer Gel in Air. *The Journal of Physics and Chemistry*, Vol. 111.
- Melcher, J. R. (1981). *Continuum Electromechanics*. Cambridge, MA: MIT Press.
- Menon, C., & Lira, C. (2006). Active Articulation for Future Space Applications Inspired by the Hydraulic System of Spiders. *Adaptation in Artificial and Biological Systems* (p. Bioinspiraton & Biomimetics). Bristol, England: Institute of Physics Publishing.
- Pearson, M. R., & Seyed-Yagoobi, J. (2008). Advances in Electrohydrodynamic Conduction Pumping. *IEEE International Conference on Dielectric Liquids*. Poitiers, France: IEEE.
- Pearson, M. R., & Seyed-Yagoobi, J. (2011). Experimental Study of EHD Conduction Pumping at the Meso- and Micro-Scale. *Elsevier, Journal of Electrostatics*, Vol. 69.
- Pearson, P. R., & Seyed-Yagoobi, J. (2011). EHD Conduction-Driven Enhancement of Critical Heat Flux in Pool Boiling. *IEEE IAS Industry Applications Society Annual Meeting*. Orlando, Florida: IEEE.
- PiezoMotor. (n.d.). *Piezo LEGS Rotary 80mNm Motor Datasheet*. Retrieved April 21, 2013, from MICROMO Micro Motion Solutions: [http://www.micromo.com/Micromo/PiezoRotatory/LEGS\\_ROTARY\\_80\\_Nmm\\_LR8012A.pdf](http://www.micromo.com/Micromo/PiezoRotatory/LEGS_ROTARY_80_Nmm_LR8012A.pdf)
- Robinson, F., Patel, V., Seyed-Yagoobi, J., & Didion, J. (2012). Terrestrial and Micro-Gravity Experimental Study of Micro-Scale Heat Transport Device Driven by Electrohydrodynamic Conduction Pumping. *Electrostatics Joint Conference*. Cambridge, ON, Canada: Electrostatics Society of America.
- Seyed-Yagoobi, J. (1999). Augmentation of Two-Phase and Single-Phase Heat Transfer and Mass Transport with Electrohydrodynamics in Thermal Equipment. *International Conference on Dielectric Liquids*. Nara, Japan: IEEE.
- Seyed-Yagoobi, J. (2005). Electrohydrodynamic Pumping of Dielectric Fluids. *Elsevier, Journal of Electrostatics*, Vol. 63.
- Sinnamon, S. (2012). Master Thesis. *Coolant Distribution Control in Satellite Structural Panels Using Electrohydrodynamic Conduction Pumping*. Albuquerque, New Mexico: The University of New Mexico.
- Takemura, K., Kozuki, H., Edamura, K., & Yokota, S. (2007). A Micromotor Using Electro-Conjugate Fluid - Improvement of Motor Performance by Using Saw-Toothed Electrode Series. *Elsevier*.

- Takemura, K., Yajima, F., Yokota, S., & Edamura, K. (2008). Integration of Micro Artificial Muscle Cells Using Electro-Conjugate Fluid. *Elsevier, Sensors and Actuators*, Vol. 144.
- Takemura, K., Yokota, S., & Edamura, K. (2005). A Micro Artificial Muscle Actuator Using Electro-Conjugate Fluid. *IEEE International Conference on Robotics and Automation*. Barcelona, Spain: IEEE.
- Wang, J., Lin, T., & Yang, L. (2007). Electrohydrodynamic (EHD) Micro-Boat. *IEEE International Conference on Nano/Micro Engineered and Molecular Systems*. Bangkok, Thailand: IEEE.
- Yokota, S., Kawamura, K., Takemura, K., & Edamura, K. (2005). A High-Integrated Micromotor Using Electro-Conjugate Fluid (ECF). *Journal of Robotics and Mechatronics*, Vol 17.

## APPENDIX A: Pump Section Construction Instructions

PLEASE READ THE FULL INSTRUCTIONS BEFORE PROCEEDING. SOME STEPS REQUIRE AN AWARENESS OF FUTURE STEPS SO THAT YOU DON'T HAVE TO GO BACK AND REDO THINGS.

Equipment:

- Deep cradle
- Shallow cradle
- 1.5" Wide teflon sheet
- 1" Wide (thin) teflon sheet
- Long 1/16th gage rod (too long to be used as a busline, but threaded at both ends)
- Heavy brass stabilizers
- 8 x high voltage electrodes
- 8 x ground electrodes
- 8 x thin spacers
- 7 x thick spacers
- 2 x busline-length 1/16th gage rods
- 1/16th gage dye for making threads
- Volt-meter for resistance measurements
- Soldering iron and solder

Note: Please wear gloves for the entirety of this process.

Double note: When the text refers to "pointing" an electrode, that means that the smaller of the two notches is "pointing" in a direction.

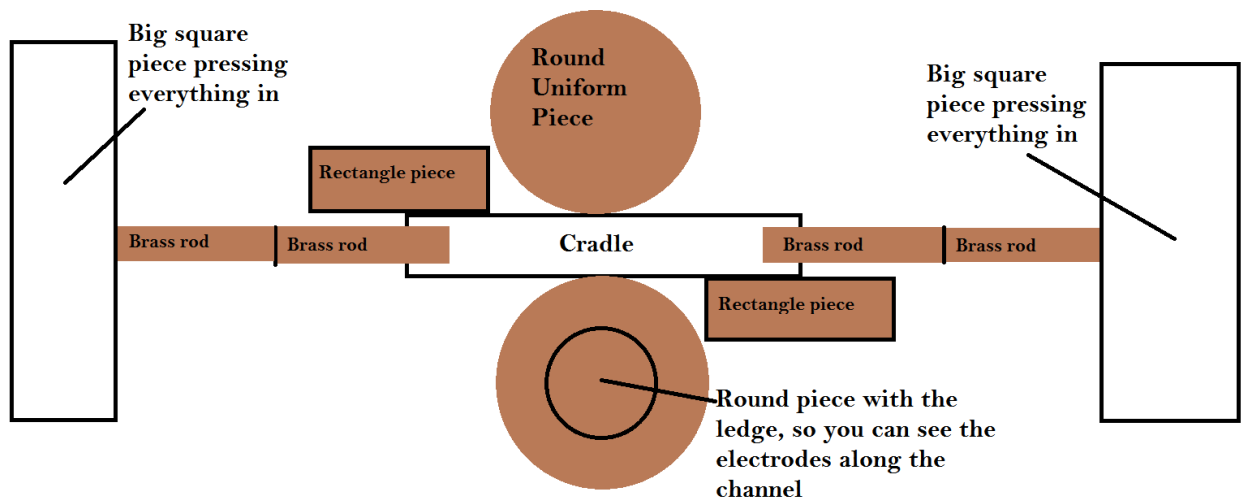
Instructions:

- 1) Cut the 2 buslines such that they stick out by about 4-6mm from either end of a teflon case (made of two end pieces and one tube middle piece). Make sure both rods are as straight as you can make them (rotate them in your hands and examine them at every angle - adjust them by bending them slightly until they're straight)
- 2) Thread both ends of the buslines about 5mm down (hold it tightly - but not too tight - in the vice such that only a bit sticks out, keep the dye as horizontal as possible)
- 3) Place the deep cradle down in the middle of the workspace and array the stabilizers around it (see attached image)
- 4) Clean with ethanol: The inside of the cradle, the teflon sheets, all the electrodes and spacers and all the 1/16th gage rods. Place all clean pieces on a clean paper towel off to the side so that nothing will contaminate them
- 5) Place the thick teflon sheet inside the cradle and tape the very ends of it down (at either end of the cradle, not in the middle)
- 6) Place the long rod at the very center of the cradle and tape it down. Note that it has to be flush against the bottom along its entire length - that's why you only tape down the very ends of the sheet in the previous step

- 7) Place all the electrodes and spacers in the channel based on this scheme: ground electrode (pointing down), thin spacer (pointing up), high voltage electrode (pointing up), wide spacer (pointing down). There should be a ground electrode at one end (say, the left end) and a high voltage electrode at the other (the right end). The sequence DOES NOT begin or end in any kind of spacer
- 8) To keep all the electrodes in place and eliminate space between them, use the stabilizer pieces to compress them from both sides
- 9) Attach a wire to one end of one of the busline rods using one of the small nuts to maintain contact. Do not use tape for this since you need a very small but very tight connection in order to not interfere with any other part of the assembly
- 10) At this point, you should be able to gently lay the busline rod down such that it is cradled by the pointing ends of all the high-voltage electrodes and thin spacers. This busline should be completely horizontal and right in the center of the cradle. If anything is crooked, adjust it now and compress the assembly to keep the new orientation. Also make sure it extends the same amount off of the electrodes at either end
- 11) Tape down the very ends of the busline you just laid down to the compressing stabilizers on either end. Do not bend the busline in order to do this - just tape it down gently to keep it straight and right in the center of the channel (it needs to stick out the same distance on either side of the electrodes stack)
- 12) Apply steel flux to the buslines and the tops of the high voltage electrodes, then carefully solder down all of the high voltage electrodes to the busline. Try to use as little solder as possible to get a good connection
- 13) Turn the volt-meter on and select the 2W (2 wire) setting - you should see 0 MOHM on the display
- 14) Connect the black prong of the volt-meter to the wire coming off of the busline
- 15) Using the red prong of the volt-meter, make sure that for all the ground electrodes the resistance is either "no reading" or some huge number in MOHMs, and make sure that for all the high-voltage electrodes it is in single OHMS (or at least <15). You can change the position of the two grenade-like stabilizers in order to achieve contact with all the high voltage electrodes
- 16) Put silicone glue inside a small, plastic syringe. Follow the next steps quickly, before the silicone hardens.
- 17) Carefully apply the silicone to the top of the channel, making sure to fill the cavities in the ground electrodes and wide spacers so that the busline rod will remain fully in place. MAKE SURE TO FULLY COVER ANY SOLDER.
- 18) Quickly run a rod (wood part of an applicator is ok) over the top of the channel such that no silicon glue protrudes from the top of the channel - it has to fit inside a tight fitting circular housing after all! There shouldn't be any bumps there that will interfere with its fit! You can also use this opportunity to try and shove any excess silicon glue into crevices that were missed in the previous step

- 19) Place the thin teflon sheet on top of the channel such that it completely covers the busline rod but still allows you to see the individual electrodes from the side.
- 20) Place the shallow cradle on top of the thin teflon sheet and place the long brass stabilizer into this cradle such that it will press down on the busline rod
- 21) Place the two big, heavy grenade-like stabilizers on top of the assembly (lean them forward onto the front stabilizer) to provide additional downward pressure
- 22) Immediately repeat the resistance testing of step 15 - adjust the grenade-likes by tiny bits if you need to. Make absolutely sure all high-voltage electrodes show a resistance of no more than ~15 OHMs.
- 23) Write up a sign telling people not to touch the assembly, the table or the drawer on the table
- 24) Leave. Come back 30 hours later
- 25) Perform the resistance testing again to make sure nothing changed/moved
- 26) Gently remove the top stabilizers, the side stabilizers the shallow channels and the teflon sheet from the assembly
- 27) Remove all the tape keeping the channel in place
- 28) Gently use a razor or other sharp blade to cut away any excess silicone that would hinder the pump's fit into its housing
- 29) Gently flip the electrodes+busline over, remove the long 1/16h gage rod from the bottom of the cradle and place the electrodes+busline back in the cradle (on top of the taped down teflon sheet), such that the recently silicon-ed busline is on the bottom
- 30) Align the bottom busline to be straight and down the center of the cradle and tape its very ends down (KEEP THE WIRE YOU CONNECTED TO IT)
- 31) Attach another wire to the second busline
- 32) Gently place the second busline on top of the channel such that it is cradled by the ground electrodes and the thick spacers. The silicon should be flexible enough to allow you to make small alignment adjustments to the electrodes and spacers should you need them. Also make sure it extends the same amount off of the electrodes at either end
- 33) Again apply flux to the busline (not to the aluminum, solder wouldn't stick to it anyway) and carefully try to create a solder bridge between the busline and each ground electrode. If you can fit the solder entirely in the cavity at the top of the electrodes, that's great – the less that's sticking out from the top of the pump the better
- 34) Repeat the resistance testing for the top busline (black prong connects to the top busline's wire, use the red prong on all the electrodes). This time make sure the ground electrodes respond with <15 OHMs and the high voltage electrodes respond with no reading or something in MOHMs. Adjust the grenade-like stabilizers as needed. You can also repeat the resistance testing for the bottom busline by simply switching the black prong to the wire coming from the bottom busline

- 35) After the resistance testing is done, silicon the top again like you did in steps 17-21. MAKE SURE ALL THE SOLDER IS COVERED
- 36) Immediately repeat the resistance testing - preferably for both top and bottom buslines
- 37) Leave. Come back 30 hours later
- 38) Take everything out of the cradle. REMEMBER WHICH SIDE THE HIGH VOLTAGE BUSLINE IS ON (DO NOT USE MARKERS OR NOTCH THE METAL. NOTCHING THE TEFLON IS OK)
- 39) Again remove any excess silicon from the outside of the round surface of the electrodes and spacers, such that they can fit into their teflon housing pieces.
- 40) Slide the entire thing first into one housing end piece, then slide the center housing piece onto it and finally another end piece. Make sure there is no torsion in the buslines and that the buslines fit through the holes in the end pieces
- 41) On the side that starts with a ground electrode, put nuts on both buslines and make sure they screw in all the way to the surface of the housing
- 42) On the other side, fit two wires onto the buslines and close them in with nuts
- 43) Attach the high-voltage connector to the high-voltage busline's wire
- 44) Done



## APPENDIX B: Final Presentation



# Electrohydrodynamic Pumping Pressure Generation

Major Qualifying Project

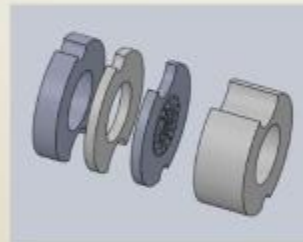
*Blair Capriotti  
Derek Montalvan  
Michal (Michelle) Talmor*

*Professor Jamal Yagoobi  
Professor Eduardo Torres-Jara  
Worcester Polytechnic Institute*



## Overview

- What is Electrohydrodynamic Pumping?
- Pressure Generation Challenge
- Methodology
- Experimental Results
- Conclusion
- Applications of the Technology
- Acknowledgements



Worcester Polytechnic Institute

- The interaction between electric fields and fluid flow fields
- Net body force equation:

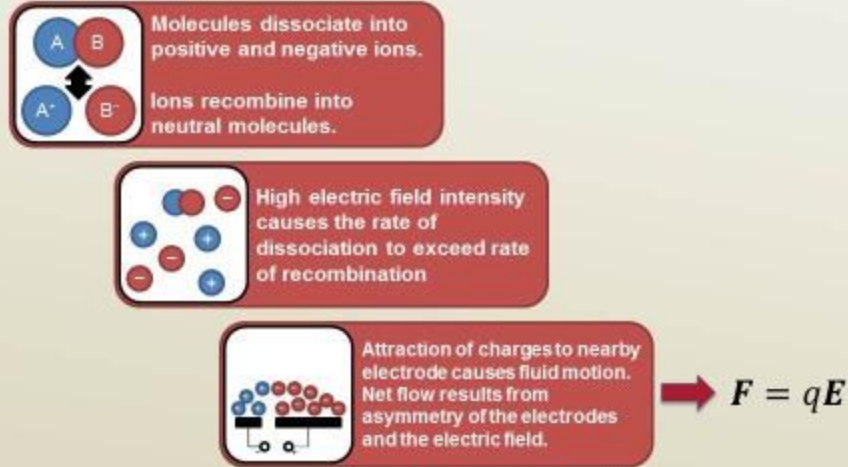
$$\mathbf{F} = q\mathbf{E} + \frac{1}{2}E^2\nabla\epsilon + \nabla\left[\rho\frac{E^2}{2}\left(\frac{\partial\epsilon}{\partial\rho}\right)_r\right]$$

 *Coulomb Force*       *Dielectrophoretic Force*       *Electrostriction Force*

Worcester Polytechnic Institute

- Ion Drag Pumping
  - Ion injection from an emitter electrode
- Induction
  - Discontinuity in fluid conductivity due to a thermal gradient
- Conduction
  - Interaction between electric field and free charges in a dielectric fluid

Worcester Polytechnic Institute

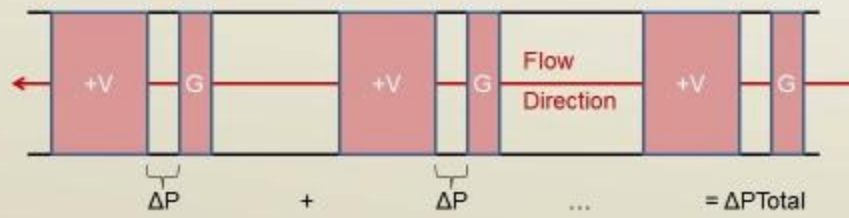


Worcester Polytechnic Institute

- Can pump thin fluid films
- Can pump vapor phases
- Works in zero gravity
- Beneficial Heat transfer applications
- No moving parts
- Small mechanism size
- Lightweight designs
- Rapid control of fluid flow
- Single & multi-phase flows
- Minimal power consumption
- Low noise, low vibrations
- Can operate in space
- Flexible configurations

Worcester Polytechnic Institute

- Sequence of pairs of asymmetric high-voltage and ground electrodes in a channel
- Generated body force between electrodes



Worcester Polytechnic Institute

- EHD pumping pressure thus far not as strong as for other pumping methods
- Challenge: Compact EHD pump design that would generate 0.3-0.5 atmosphere
  - Estimation of possible pressure range
  - Innovative electrode & housing design
  - Experimental setup design

Worcester Polytechnic Institute

- Numerical estimation of pressure
- Selection of working fluid & number of electrodes
- Electrode pair dimensions and design
- Pump sections & Housing design
- Experimental setup design
- Material selection
- Manufacturing & Construction
- Experiment overview

Worcester Polytechnic Institute

- Pressure is proportional to the square of the electric field strength<sup>[4]</sup>:

$$P \approx \epsilon E^2$$

$\epsilon$  = electric permittivity of working fluid

$$E = V/L$$

V = Voltage    L = Space between electrodes

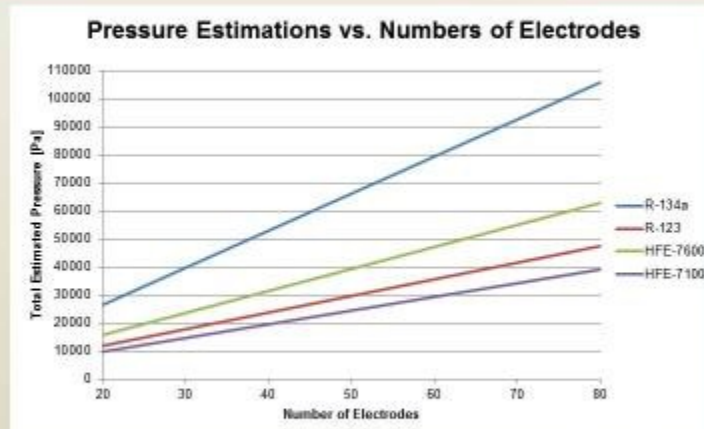
- Working fluid properties greatly affect generated pressure

Worcester Polytechnic Institute

- Fluid Candidates<sup>[5]</sup>:

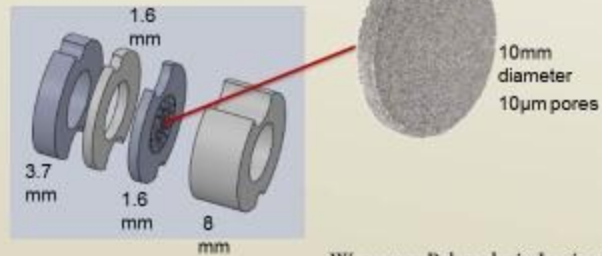
Fluid Name	Dielectric Constant	Conductivity [S/m]	Density [kg/m <sup>3</sup> ]	Boiling point [C]	Dielectric Strength [kV/mm]
HFE 7600	6.4	3.33E-08	1540	98	31 kV
HFE 7100	7.4	7.0E-10	1520	61	11 kV
R-123	4.8	2.7E-8	1464	27	25 kV
R-134a	9.51	5.65E-11	1233	-26	18 kV

- HFE 7600 chosen

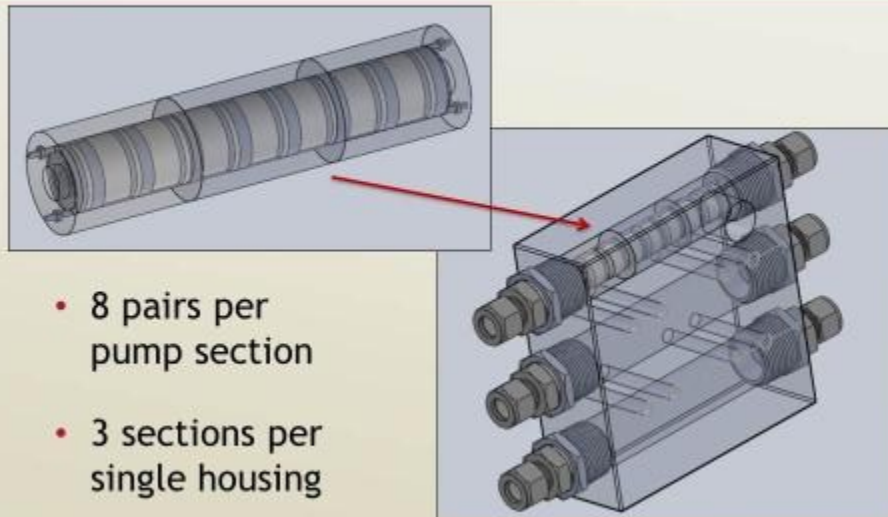


- 72 electrodes chosen (safety factor of 1.2)

- Porous/Permeable High Voltage Electrodes:
  - Best Pressure Generation Performance<sup>[6,7]</sup>
- Flush Ring Ground Electrodes
  - Avoid hindrance of the flow



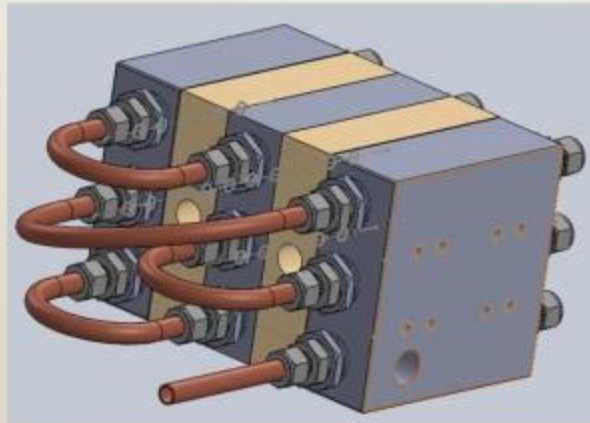
Worcester Polytechnic Institute



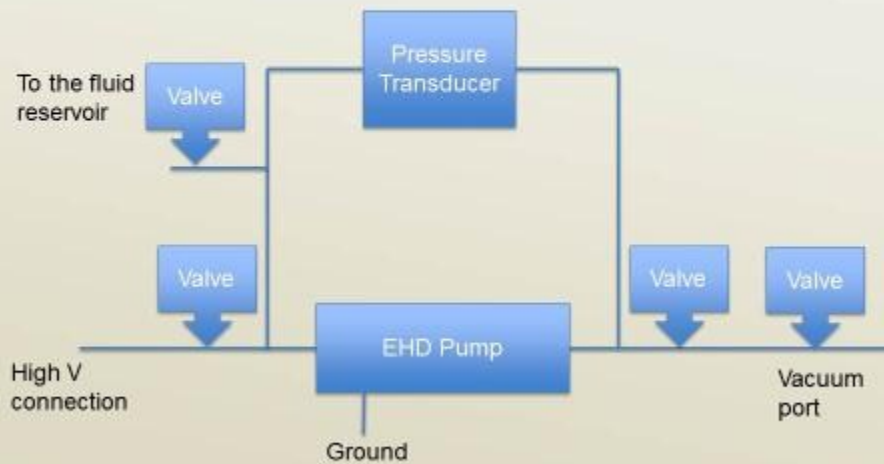
- 8 pairs per pump section
- 3 sections per single housing

Worcester Polytechnic Institute

- Total of 9 pump sections



Worcester Polytechnic Institute

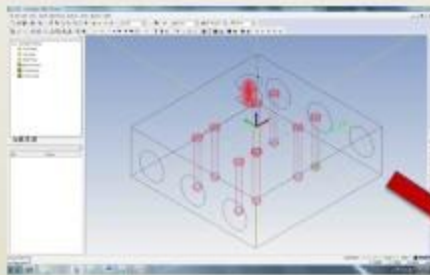


Worcester Polytechnic Institute

- Electrodes
  - Stainless steel
  - Aluminum
- Insulator pieces
  - Teflon or PTFE
- Housing
  - Aluminum
- Connectors & Tubing
  - Copper and brass

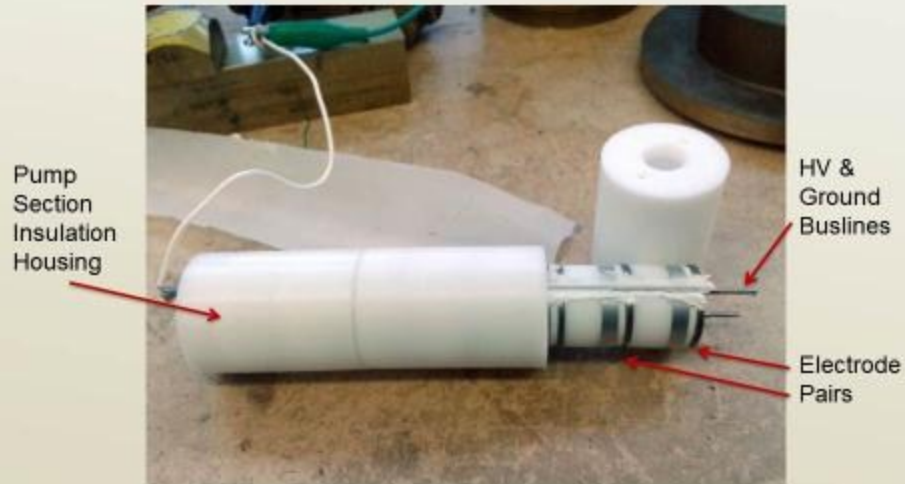
**All compatible with  
the working fluid!**

Worcester Polytechnic Institute

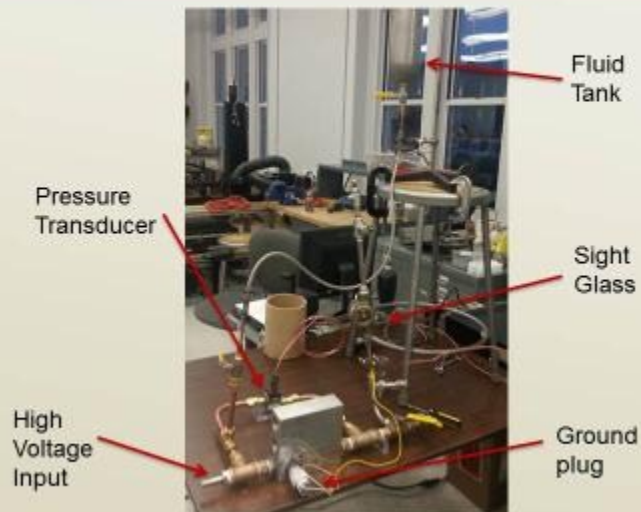


- From SolidWorks to Esprit
- Manufacturing programming
- Lathe & CNC machining

Worcester Polytechnic Institute



Worcester Polytechnic Institute



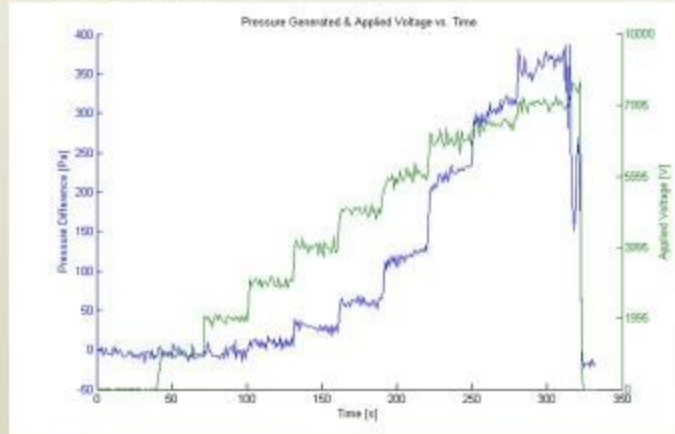
Worcester Polytechnic Institute

- Single pump section
  - HFE-7600
  - R-123
- Remaining pump sections in a single housing piece
- All remaining housing pieces

- DAQ Board & LabVIEW
  - 10 samples per second
  - Time, Differential Pressure, Voltage, Current

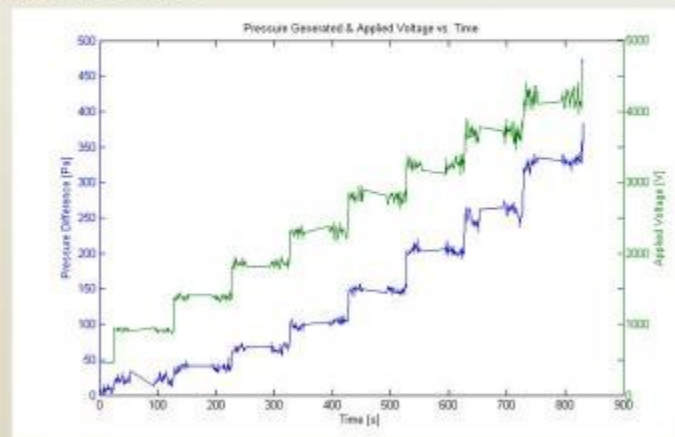


- Initial results:



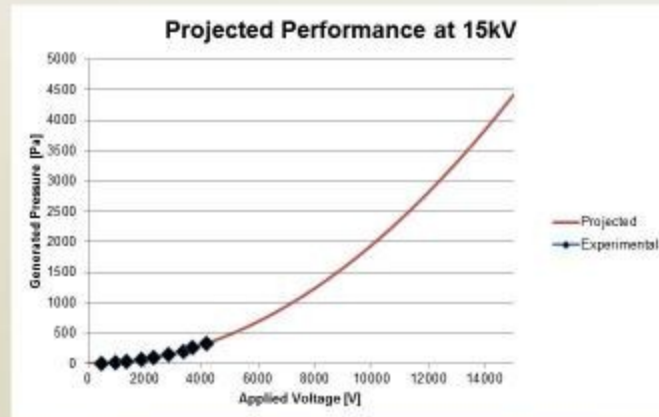
Worcester Polytechnic Institute

- Final Results



Worcester Polytechnic Institute

- Projected Results



Worcester Polytechnic Institute

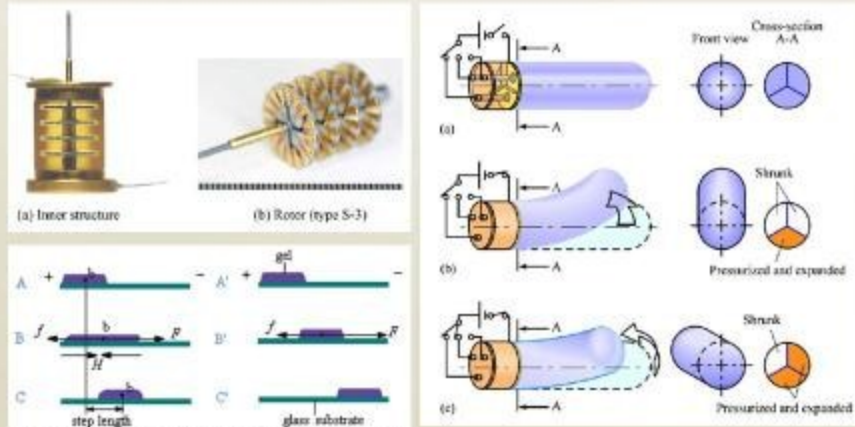
- Sealing and leak detection
- Electric resistance & contact
- Choice of materials
- Manufacturing constraints
- Presence of air

Worcester Polytechnic Institute

- Ambitious design
- Complex task, limited time
- Promising results
- Additional tests must be performed
- 2013 IEEE IAS Annual Meeting in Orlando, FL

- Hydraulic Actuation for Autonomous Devices
  - EHD effects increase in smaller scale
  - Simple printed circuits
  - High estimated pressure capabilities<sup>[8]</sup>
  - Reliable control schemes
- Thermal Control of Autonomous Electronics
  - Cooling system for robotic satellite systems<sup>[9]</sup>
  - Smart skin systems via distribution control<sup>[10]</sup>

- Sample Applications<sup>[11,12,13]</sup>



Worcester Polytechnic Institute

## Acknowledgements

- We would like to thank Professors Yagoobi & Torres-Jara, as well as Viral Patel & Lei Yang of the Mechanical Engineering Department, for all of their help and guidance
- We would like to also extend thanks to the Washburn Shops for aiding in the manufacturing process
- Lastly, we would like to mention our excellent vendors:



**Howard Products Sheet Metal**  
Precision Sheet Metal Fabrication

Worcester Polytechnic Institute

1. *Electrohydrodynamic Pumping of Dielectric Liquids*, Jamal Seyed-Yagoobi, *Journal of Electrostatics* 63, 2005
2. *Experimental Study of EHD Conduction Pumping at the Meso- and Micro-Scale*, Matthew R. Pearson, Jamal Seyed-Yagoobi, *Journal of Electrostatics* 65, 2011
3. *Electrohydrodynamically Induced Dielectric Liquid Flow Through Pure Conduction in Point/Plane Geometry*, P. Atten, J. Seyed-Yagoobi, *IEEE Transactions on Dielectrics and Electrical Insulation*, Vol. 10, No. 1, 2003
4. *Understanding of Electrohydrodynamic Conduction Pumping Phenomenon*, Yinshan Feng, Jamal Seyed-Yagoobi, *Physics of Fluids*, Vol. 16, No. 7, 2004
5. *ASHRAE Handbook - Fundamentals, Refrigerants*, American Society of Heating, Refrigeration and Air-Conditioning Engineers, Inc., 2005
6. *Advances in Electrohydrodynamic Conduction Pumping*, Matthew R. Pearson, Jamal Seyed-Yagoobi, *IEEE Transactions on Dielectrics and Electrical Insulation*, Vol. 16, No. 2, 2009
7. *Innovative Electrode Designs for Electrohydrodynamic Conduction Pumping*, Seong-Il Jeong, Jamal Seyed-Yagoobi, *IEEE Transactions on Dielectrics and Electrical Insulation*, Vol. 40, No. 3, 2004
8. *Micro-Scale Electrohydrodynamic Pumped High Performance Actuation*, R. Keshari, S. Kang, K. P. Hallinan, *Journal of Intelligent Material Systems and Structures*, Technomic Publishing Co., Inc., Vol 11, 2001
9. *Coolant Distribution Control in Satellite Structural Panels Using Electrohydrodynamic Conduction Pumping*, Samuel Sivanon, Master of Science Thesis Submission, The University of New Mexico, 2012
10. *Control of Liquid Flow Distribution Utilizing EHD Conduction Pumping Mechanism*, Yinshan Feng, Jamal Seyed-Yagoobi, *Industry Applications Conference, 39th IEEE IAS Annual Meeting Conference Record*, 2004
11. *A Micromotor Using Electro-Conjugate Fluid - Improvement of Motor Performance by Using Saw-Toothed Electrode Series*, K. Takemura, H. Kozumi, K. Edamura, S. Yokota, Elsevier, 2007
12. *Biologically Inspired Path-Controlled Linear Locomotion of Polymer Gel in Air*, S. Liang, J. Xu, L. Wang, L. Zhang, X. Guo, X. Zhang, *Journal of Physics B: Chemistry*, American Chemical Society, 2007
13. *Concept of a Micro Finger Using Electro-Conjugate Fluid and Fabrication of a Large Model Prototype*, R. Abe, K. Takemura, K. Edamura, S. Yokota, Elsevier, 2006

Worcester Polytechnic Institute

# QUESTIONS?

Worcester Polytechnic Institute